CEN

WORKSHOP

AGREEMENT

CWA 18011

July 2023

ICS 77.140.20

English version

Guidelines for the evaluation of the plane stress fracture toughness of advanced high strength steel sheets in the frame of fracture mechanics

EUROPEAN COMMITTEE FOR STANDARDIZATION
COMITÉ EUROPÉEN DE NORMALISATION
EUROPÄISCHES KOMITEE FÜR NORMUNG

CEN-CENELEC Management Centre: Rue de la Science 23, B-1040 Brussels

Ref. No.:CWA 18011:2023 E

Contents

Page

European foreword 3
Introduction 4
1 Scope 5
2 Normative references 6
3 Terms and definitions 6
4 Symbols and abbreviations 8
4.1 Symbols 8
4.2 Abbreviations 8
5 Fracture toughness evaluation of thin ductile metal sheets 9
5.1 J-integral 9
5.2 CTOA and δ_5 13
5.3 Kahn-type tear tests 15
5.4 Essential Work of Fracture 16
5.4.1 Essential Work of Fracture methodology 16
5.5 Summary of fracture toughness testing methods 29
6 Fracture toughness: a key material property for material design 30
6.1 Fracture toughness in engineering materials design 30
6.1.1 Microstructural optimization 30
7 Fracture toughness measurements for material selection 32
7.1 Fracture toughness to select materials with improved cracking resistance 32
7.2 Classification according to cracking resistance 36
7.3 Rapid fracture testing methods for material screening 37
8 Fracture toughness measurements for quality control of raw materials 38
9 Application of fracture toughness measurements in production: Industrial case studies 40
Bibliography 43

European foreword

This CEN Workshop Agreement (CWA 18011:2023) has been developed in accordance with the CEN-CENELEC Guide 29 "CEN/CENELEC Workshop Agreements – A rapid prototyping to standardization" and with the relevant provisions of CEN/CENELEC Internal Regulations – Part 2. It was approved by a Workshop of representatives of interested parties on 2023-05-17, the constitution of which was supported by CEN following the public call for participation made on 2022-08-03. However, this CEN Workshop Agreement does not necessarily include all relevant stakeholders.

The final text of this CEN Workshop Agreement was provided to CEN for publication on 2023-06-19.

This CEN Workshop Agreement is based on the results of the ToughSteel research project, which received funding from the Research Fund for Coal and Steel under grant agreement Nº 101034036.

The following organizations and individuals developed and approved this CEN Workshop Agreement:

— EURECAT, Spain, (Project leadership), Dr. David Frómeta, Dr. Daniel Casellas, Mr. Sergi Parareda, Ms. Laura Grifé, , Ms. Marina Presas, , Mr. Toni Lara

— UNE, Spain, Mr. Javier López-Quiles (Secretary)

— Université catholique de Louvain, Belgium, Dr. Pierre Bollen, Dr. Marie-Stéphane Colla, Dr. Antoine Hilhorst, Prof Pascal J. Jacques, Prof. Thomas Pardoen.

— CIEMAT, Spain, Ms. Marta Serrano, Mr. Antonio Fernández

— OCAS NV, Belgium, Dr. Okan Yilmaz

— APERAM, France, Mr. Xavier Boyat

Attention is drawn to the possibility that some elements of this document may be subject to patent rights. CEN-CENELEC policy on patent rights is described in CEN-CENELEC Guide 8 "Guidelines for Implementation of the Common IPR Policy on Patent". CEN shall not be held responsible for identifying any or all such patent rights.

Although the Workshop parties have made every effort to ensure the reliability and accuracy of technical and non-technical descriptions, the Workshop is not able to guarantee, explicitly or implicitly, the correctness of this document. Anyone who applies this CEN Workshop Agreement shall be aware that neither the Workshop, nor CEN, can be held liable for damages or losses of any kind whatsoever. The use of this CEN Workshop Agreement does not relieve users of their responsibility for their own actions, and they apply this document at their own risk. The CEN Workshop Agreement should not be construed as legal advice authoritatively endorsed by CEN/CENELEC.

Introduction

Fracture toughness, from a fracture mechanics point of view, is the property that controls the crack initiation and propagation resistance of a material. It is important to differentiate this definition from the conventional use of the term 'toughness', referring to the area under the stress-strain curve of a uniaxial tensile test or the product of the ultimate tensile strength by the total elongation (UTS × TE), which is not suitable to describe the material resistance in the presence of pre-existing cracks or defects.

Fracture toughness of ductile engineering materials can be measured in the frame of Elastic-Plastic Fracture Mechanics (EPFM) following the *J*-integral (giving the value of J_C), the J-R curve or the CTOD procedures standardized in ASTM E1820 [1] and ISO 12135 [2]. However, these standard methods are intended to characterize the plane strain fracture toughness of metallic materials and, therefore, the defined thickness requirements are not satisfied by thin sheets, such as the sheets used in the automotive industry (1-3 mm). Alternative standards were developed later for the evaluation of the resistance to stable crack extension of thin-gauge materials, the ASTM E2472 [3] and the ISO 22889 [4]. These standards propose the use of alternative parameters for fracture resistance characterization, the Crack Tip Opening Angle (CTOA) and the crack opening displacement δ_5. These standard methods are experimentally complex, they require expert technical skills for specimen preparation and the crack advance must be monitored during the whole test, which represents one of the main challenges in fracture mechanics testing procedures. Additionally, they usually involve complex data processing and, such as in the case of the CTOA fracture criterion, the use of finite element method analysis, which makes the application of the methods expensive and time-consuming. Thus, alternative simpler and faster experimental approaches, such as the Essential Work of fracture (EWF) methodology [5] or the Kahn-type tear tests [6], have been developed in order to satisfy the growing need of knowing the fracture properties of thin metallic sheets.

Nevertheless, there are still some uncertainties regarding which are the most suitable testing methods to assess the plane stress fracture toughness of high strength metal sheets and the meaning of the evaluated fracture parameters. The present CWA reviews and discusses some of the different existing experimental approaches to evaluate the fracture toughness of thin ductile sheets and explores their application to better understand the formability and crashworthiness of advanced high strength steel (AHSS) sheets. The aim is to provide some guidelines that contribute to a more efficient fracture resistance and crashworthiness prediction in different industrial applications.

1 Scope

This CWA provides information of interest about the fracture toughness evaluation of thin high strength metal sheets and its implication on sheet metal formability and crashworthiness. The document summarizes the most relevant findings obtained in previous research projects and academic works (PhD theses, post-doc works, scientific publications).

The main experimental methodologies to characterize the plane stress fracture toughness of thin ductile metal sheets are described and analysed in terms of complexity, accuracy and quickness. The most relevant fracture toughness parameters are defined, and a compilation of standard testing procedures is given.

Furthermore, the document includes recommendations to be applied during the different stages of AHSS manufacturing, from the microstructural design to the implementation in cold-formed components. Different examples are shown on how fracture toughness measurements can help to predict formability and part performance. Additionally, successful industrial case studies, where fracture toughness measurements have been used to solve cracking related issues in cold-formed components are reported to better exemplify the benefits of using a fracture mechanics approach in the design and implementation of AHSS sheets. The structure of the CWA is schematized in Figure 1.

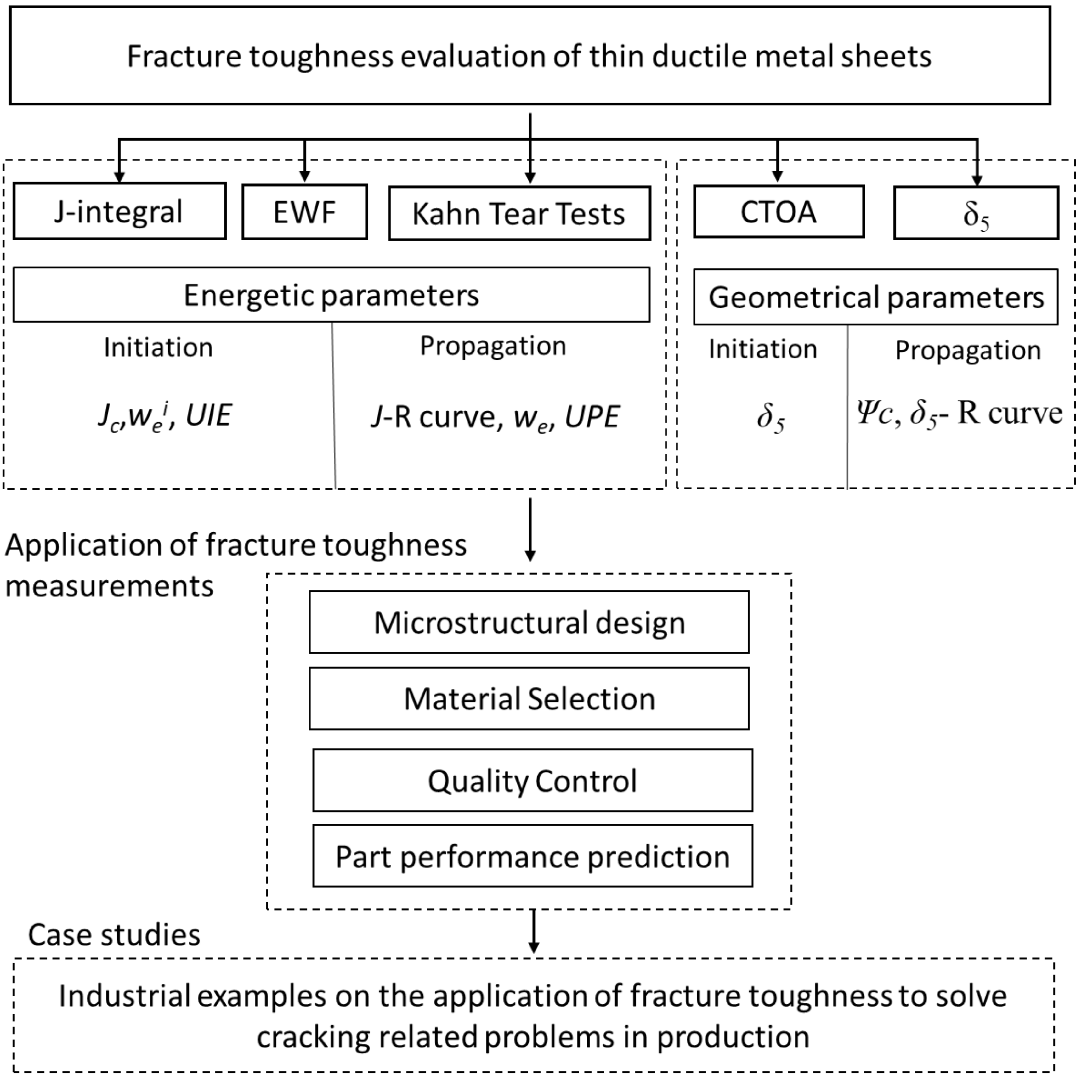

Figure 1 — Structure of the user guideline for the application of fracture toughness to understand crack-related problems in high strength metal sheets

2 Normative references

There are no normative references in this document.

3 Terms and definitions

For the purposes of this document, the following terms and definitions apply.

ISO and IEC maintain terminology databases for use in standardization at the following addresses:

— ISO Online browsing platform: available at https://www.iso.org/obp/

— IEC Electropedia: available at https://www.electropedia.org/

3.1
fracture process zone
FPZ
end region ahead of the crack tip

3.2
total work of fracture
W_f
energy obtained from integration of the area under the load-displacement curve for the complete fracture

3.3
essential work of fracture (EWF)
W_e
energy dissipated in the fracture process zone

3.4
non-essential plastic work
W_p
energy dissipated in the outer region surrounding the fracture process zone associated with plastic deformation

3.5
specific work of fracture
w_f
total fracture energy per unit area

3.6
specific essential work of fracture
w_e
energy dissipated in the fracture process zone per unit area

3.7
specific non-essential plastic work
w_p
plastic energy dissipated in the outer region surrounding the fracture process per unit volume

3.8
specific work of fracture initiation
$w_f{}^i$
crack growth initiation energy per unit area for a determined specimen

3.9
specific essential work of fracture initiation
$w_e{}^i$
initiation toughness obtained from an average of $w_f{}^i$ values

3.10
crack opening displacement
COD
force induced separation vector between two points at a specific gage length. The direction of the vector is normal to the crack plane

3.11
crack tip opening displacement
δ
the crack displacement resulting from the total deformation (elastic plus plastic) at variously defined locations near the original crack tip

3.12
crack tip opening angle
ψ
relative angle of the crack surfaces measured at 1 mm from the current crack tip

3.13
critical crack tip opening angle
ψ_c
steady-state value of crack tip opening angle ψ at 1 mm from the current crack tip

3.14
J-integral
line or surface integral that encloses the crack front from one crack surface to the other and characterizes the local stress-strain field at the crack tip

3.15
J-Resistance curve
J-R curve
variation of J with stable crack extension

3.16
unit initiation energy
UIE
the amount of energy required to initiate a crack in a tear specimen divided by the by the original net area of the specimen. Initiation energy is determined by integrating the area under the load-displacement curve from the beginning of the test to the point of maximum load

3.17
unit propagation energy
UPE
the amount of energy required to propagate a crack in a tear specimen divided by the original net area of the specimen. Propagation energy is determined by integrating the area under the load-displacement curve from the point of maximum load to the point of complete fracture

4 Symbols and abbreviations

4.1 Symbols

A_{pl}	Area under the load – displacement curve for J-integral calculation
β	Plastic zone shape factor
δ_5	Crack opening displacement over a 5 mm gauge length at tip of fatigue pre-crack
δ_c	Critical crack opening displacement
J_c	J-integral value near the onset of stable crack propagation (plane stress, thickness dependent)
J_{Ic}	J-integral value near the onset of stable crack propagation (plane strain, thickness independent)
K_{Ic}	Mode I plane strain fracture toughness. Linear Elastic Fracture Mechanics
l_o	Original uncracked ligament length
ψ	Crack Tip Opening Angle.
ψ_c	Critical Crack Tip Opening Angle
σ_y	Effective yield strength
t_o	Original specimen thickness
W_f	Total Work of Fracture
W_e	Essential Work of Fracture
W_p	Non-essential plastic Work
w_f	Specific total work of fracture
w_e	Specific essential work of fracture
$w_f{}^i$	Specific work of fracture initiation
$w_e{}^i$	Specific essential work of fracture initiation

4.2 Abbreviations

AHSS	Advanced High Strength Steels
CI	Crash Index
CIDR	Crash Index Decreasing Rate
CRI	Cracking Resistance Index

CTOA	Crack Tip Opening Displacement
CT	Compact Tension
CTOD	Crack Tip Opening Angle
CP	Complex Phase
CWA	CEN Workshop Agreement
DENT	Double Edge Notched Tension
DP	Dual Phase
ESIS	European Structural Integrity Society
EWF	Essential Work of Fracture
FPZ	Fracture Process Zone
HER	Hole Expansion Ratio
PHS	Press Hardened Steel
RA	Retained Austenite
SENB	Single Edge Notched Bending
TE	Total Elongation
TFS	True Fracture Strain
TRIP	Transformation Induced Plasticity
TTS	True Thickness Strain
UIE	Unit Initiation energy
UPE	Unit Propagation Energy
UTS	Ultimate Tensile Strength
YS	Yield Stress

5 Fracture toughness evaluation of thin ductile metal sheets

5.1 J-integral

ASTM E1820 [1] and ISO 12135 [2] describe in detail the specimens and tests characteristics for the evaluation of fracture toughness of metallic materials using the parameters, *J* and CTOD (δ). The standard establishes two procedures: a basic procedure for the direct evaluation of a single *J* or CTOD value and a procedure to determine the fracture toughness resistance (*R*) curve (*J*-*R* curve). The experimental procedures described in the two standards are similar but there are some variations in data treatment and qualified data criteria, which can affect the calculation of J_{Ic} [7].

The basic procedure allows obtaining a single fracture toughness value such as J_{Ic} or δ_{Ic}. Multiple specimens are used to evaluate *J* at crack initiation, J_{Ic}. The initial and final crack sizes are measured by optical measurements. On the other hand, the resistance curve procedure uses an elastic unloading procedure to obtain a *J* or CTOD-based resistance curve from a single specimen. In this procedure, the crack length is measured from compliance and is verified by optical measurements. Specimens recommended are the Compact Tension (CT) and the Single Edge Notched Bending (SENB).

In materials showing a rising *R* curve behaviour, J_c has shown to be a very conservative parameter to evaluate the fracture toughness and, thus, the complete *J*-*R* curve must be determined. However, it is also

important to note that, even though J_{IC} values are independent of specimen geometry, the *R* curve is influenced by the constraint level at the crack tip, and therefore it depends upon specimen geometry [8-10].

An example of a *J-R* curve determination with a CT specimen according to ASTM E1820 is shown in Figure 2. The specimen is loaded and subjected to successive partial unloading cycles. The slopes provide a measure of the elastic stiffness of the specimen, which decreases as the crack grows and allows estimating the crack length at different points during the test.

The *J* values are calculated for the different points along the load - displacement curve. The area under the load - displacement curve, A_{pl}, is required to evaluate *J*. Such area represents the area under the load vs displacement curve for the load and unload of a hypothetic crack length $a = a_i + \Delta a$, where a_i is the initial crack length and Δa the crack extension. Thus, the hypothetic load slope for m_5 is lower than the initial slope m_i (Figure 2).

The *J* value can be determined by:

$$J = J_{\text{el}} + J_{\text{pl}} \tag{1}$$

where

J_{el} and J_{pl} are the elastic and the plastic component of *J*, respectively and are given by:

$$J_{el} = \frac{K^2\left(1-\vartheta^2\right)}{E} \tag{2}$$

$$J_{pl} = \frac{\eta A_{pl}}{B(W-a)} \tag{3}$$

where

$\eta = 2 + \frac{0{,}522\left(W-a\right)}{B}$ for the CT specimen;

B and *W* are the specimen thickness and width respectively;

a is the crack size.

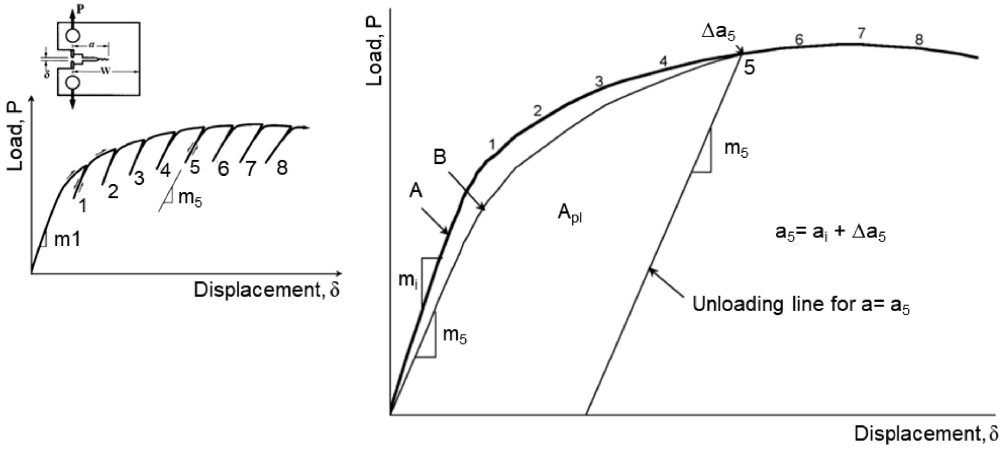

a) **b)**

Figure 2 — a) *J* determination through partial unloading cycles following the compliance method; b) Plastic area, A_{pl}, to calculate the *J*-integral. The curve A represents the actual load-displacement curve of the growing crack. The curve B corresponds to the hypothetic load-displacement curve for a stationary crack with length a_5 [11]

The *J* values are plotted against the crack extension, Δ*a*, in order to obtain the *J-R* curve (Figure 3). The process for the construction of the *J-R* curve is described as follows:

A construction line is drawn with slope $2\sigma_Y$, where:

$$\sigma_y = \frac{\sigma_{ys} + \sigma_{UTS}}{2} \tag{4}$$

Such slope represents the initial slope caused by the blunting of the crack tip. Two exclusion lines parallel to the construction line are plotted at 0,15 mm and 1,5 mm. The data points lying between these two lines define the *J-R* curve. The J_Q value, which characterizes the fracture toughness at the onset of the crack propagation is determined by the intersection of the *J-R* curve with a third line, parallel to the exclusion lines, drawn at 0,2 mm. The boundary J_{limit} is given by the smaller of the following:

$$J_{\max} = b_o \ \sigma_y \ / \ 10 \tag{5}$$

or

$$J_{\max} = B \ \sigma_y \ / \ 10 \tag{6}$$

where

b_O is the distance from the original crack front to the back edge of the specimen, i.e. the initial ligament length;

B is the thickness of the specimen.

The maximum crack extension capacity for a specimen is:

$$\Delta a_{\max} = 0,25 b_o \tag{7}$$

In order that J_Q can be considered as the size-independent plane-strain fracture toughness, J_{IC}, the following conditions must be satisfied:

$$B, b_0 > 10\frac{J_Q}{\sigma_Y} \tag{8}$$

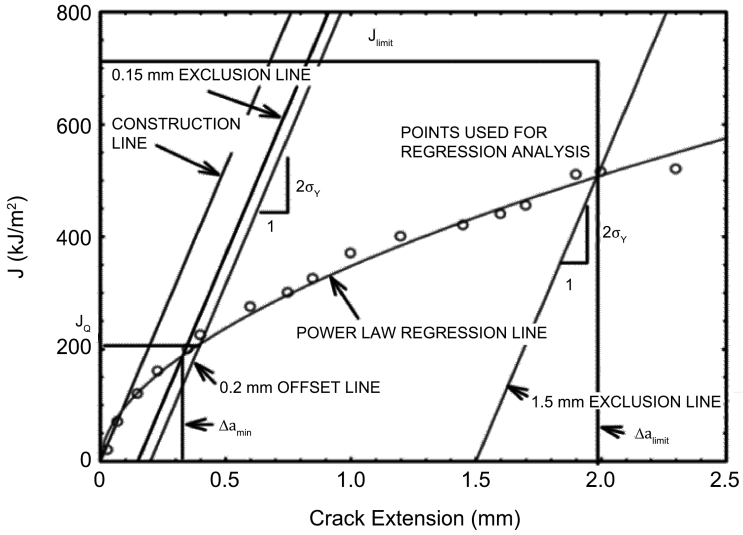

Figure 3 — J -R curves and construction lines for data qualification according to ASTM E1820[1]

Unfortunately, the standard methods defined in ASTM E1820 and ISO 12135 cannot be directly applied to thin sheet materials because of their minimum specimen size requirements. For example, considering a thickness of 1,5 mm and the proportions given in ASTM E1820 for a Compact Tension (CT) specimen ($2 \leq W/B \leq 4$, where W is the distance between the load line and the back end of the specimen and B is the sheet thickness), a specimen with a maximum size of 7,2 × 7,5 mm could be used, which would severely hamper its manipulation and testing.

However, several authors have demonstrated that if the thickness limitations are disregarded, it is possible to use the *J*-integral procedure to evaluate the *J*-*R* curve of ductile sheet materials [10, 12]. Some authors have used alternative specimen geometries and J-integral expressions to evaluate the critical *J* value at crack initiation (J_C) of thin metal sheets [10, 13-16].

Reported J_C values for thin metal sheets are shown in Table 1. It is important to note that J_C values of thin ductile sheets under plane stress conditions have a significant contribution from necking and, thus, J_C depends upon specimen thickness. It is recommended to use the notation J_C to avoid confusion with the thickness-independent plane strain fracture toughness J_{IC}. In order to consider $J_C = J_{IC}$, the conditions given in Equation 8 must be satisfied.

Table 1 — Published J_C values for metal sheets

Material	Thickness [mm]	J_C [KJ/m^2]
Low C steel (no specific % C) [15]	2,0	510
TRIP steel (8 % austenite vol. fraction) [13]	0,9	225
TRIP steel (24 % austenite vol. fraction) [13]	0,9	45
Aluminium 6082 T0 [16]	1,0-6,0	50-150
TWIP steel [14]	1,45	250
Dual-Phase steel [14]	1,85	100
Quenching & Partitioning steel [14]	1,0	65
Dual Phase [10]	1,4	158
TRIP-aided Bainitic Ferritic [10]	1,5	157
Quenching & Partitioning steel [10]	1,4	280
Complex Phase [10]	1,4	286

5.2 CTOA and δ_5

ASTM E2472 [3] and ISO 22889 [4] describe the experimental procedure for determining the crack opening displacement δ_5 and the crack tip opening angle ψ in thin compact and middle-crack tension specimens. δ_5 is the relative displacement of the crack surfaces normal to the original crack plane at the crack tip, measured on the specimen surface over an initial gauge length of 5 mm. The δ_5 results are expressed in terms of a resistance curve (δ_5-R).

The standards define ψ as the relative angle of the crack surfaces measured at 1 mm from the current crack tip. The critical CTOA, ψ_C, is expressed in terms of a constant value achieved after a certain amount of crack extension. Figure 4 shows an example of the specimen geometry and the procedure for determining ψ_C.

The CTOA is directly measured on the specimen surface with an optical microscope or by digital image correlation equipment. The CTOA values are represented as a function of the crack extension, as illustrated in Figure 4. After the initiation of propagation, the CTOA gradually decreases until it reaches a steady value during stable tearing. The average of the CTOA values in this constant region corresponds to the ψ_C. The maximum amount of crack extension, Δa_{max}, is given by:

$$\Delta a_{max} = (W - a_0) - 4B \tag{9}$$

where

W is the specimen with;

a_0 is the initial crack length;

B is the specimen thickness.

The minimum amount of crack extension, Δa_{min}, is that for which the CTOA reaches the constant value.

Alternative methods for CTOA determination are proposed in the ISO 22889, such as post-test microtopography measurements, finite element analysis and indirect determination using δ_5.

Table 2 shows published values of ψ_C for different sheet materials.

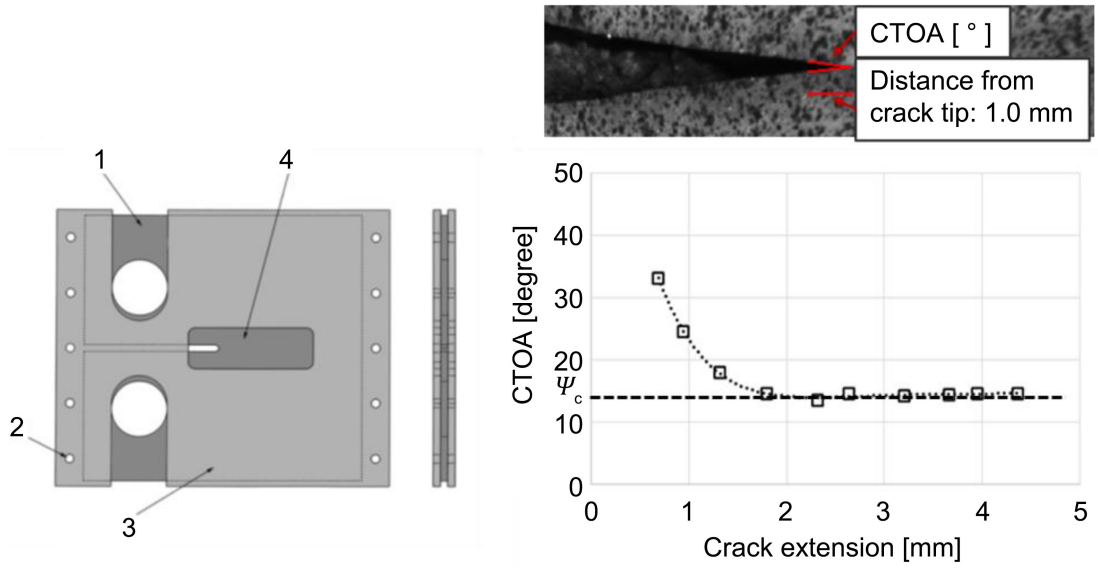

a) **b)**

Key

1 C(T) specimen
2 bolt holes
3 anti-buckling plates (front and back)
4 crack viewing region

Figure 4 — a) Compact tension specimen with an anti-buckling system [4] and b) example of CTOA and ψ_C determination by direct optical measurements

Table 2 — ψ_C values for different sheet materials

Material	Thickness [mm]	ψ_C [°]
AA2024-T3 [17]	2,3	5,8
AA 5083 [18]	3,0	5
Interstitial free high strength (IFHS) steel [19]	1,0	12
Dual Phase steel 780 [20]	1,6	8,6
Dual Phase steel 980 [20]	1,94	3,6
API 5L X65 pipe steel [21]	6,0	20

5.3 Kahn-type tear tests

The Kahn-type tear test was developed by Kaufman and Knoll [6] to characterize the notch resistance of thin aluminium sheets. The test consists in pulling at constant speed a sharp-notched specimen and recording the load as a function of the displacement. Figure 5 shows the typical load-displacement curve of these tests. The Unit Initiation Energy, *UIE*, represents the notch resistance to nucleate a crack and is calculated from the area under the curve at maximum load. The Unit Propagation Energy, *UPE*, represents the crack propagation resistance of the material. The ASTM B871 [22] standard describes the experimental procedure for obtaining the *UIE* and *UPE* in thin aluminium alloy sheet products. The *UPE* is the primary result of the test and it can be used as a relative fracture toughness indicator. Some works have shown a good correlation between *UPE* and K_{IC} [6, 23].

The method has been used in many research works to characterize the toughness of aluminium alloys [6, 23-25] and high strength steels [10, 26-28]. The method is very interesting because of its high simplicity but it has its limitations. As discussed in [10], while *UIE* values may be suitable enough to estimate crack initiation resistance by means of the *UIE*, *UPE* values completely overestimate crack propagation resistance, since they include an energetic contribution from plasticity. Therefore, *UPE* cannot be considered a geometry-independent property. On the other hand, it has been shown that it may provide misleading fracture toughness estimations and inappropriate material ranking [10].

Table 3 shows some reported values of *UIE* and *UPE* for different aluminium alloys and steels.

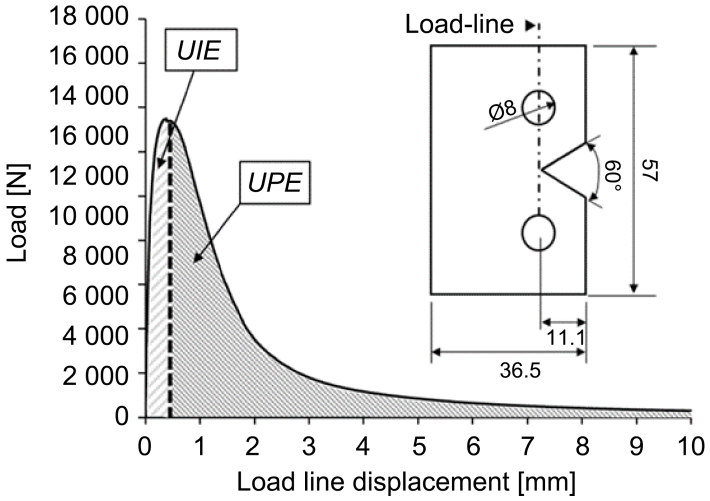

Figure 5 — Typical specimen geometry and load-displacement curve of a Kahn Tear Test [10]

Table 3 — *UIE* and *UPE* values for different aluminium alloy and steel sheets

Material	*UIE* [kJ/m^2]	*UPE* [kJ/m^2]
AA7050 Al alloy [78]	20-160	Not reported
EN AW-6xxx C [79]	Not reported	280
EN AW-6xxx HS [79]	Not reported	115
Hot stamped 22MnB5 [80]	400-480	Not reported
TWIP steel [81]	400-440	1 180-1 350
Dual Phase [10]	87	479
TRIP-aided Bainitic Ferritic [10]	104	579
Quenching & Partitioning steel [10]	144	566
Complex Phase 1 000 MPa [10]	147	639
Complex Phase 1 200 MPa [28]	123	377
TBF/Q&P 1 000 MPa [28]	119	755
PHS 1 500 [28]	115	448
PHS1 000 [28]	123	494

5.4 Essential Work of Fracture

5.4.1 Essential Work of Fracture methodology

The Essential Work of Fracture (EWF) methodology has been established as one of the most interesting methods to characterize the fracture resistance of thin ductile sheets. The main advantage of this technique is its relative experimental simplicity compared to other conventional fracture mechanics procedures since it does not require crack growth monitoring and data post-processing is rather simple. The EWF method was originally developed by Cotterell and Reddel for ductile metals [5] and was rapidly extended for the characterization of ductile polymers [29-31]. Over the years, the methodology has been widely used for evaluating the fracture resistance of polymer films [32-35] and metallic materials: low carbon steels [36, 37], aluminium alloys [16, 37-40], zinc [39], copper [41] and brass [42]. More recently, the method has gained increasing interest to characterize the fracture resistance of high strength steel sheets. Lacroix et al. [13] used the EWF to evaluate the fracture toughness of different TRIP-assisted steels and to investigate the influence of the TRIP effect on their crack propagation resistance. Later, Muñoz et al. [43] and Gutiérrez et al. [44] studied the applicability of the method in various AHSS steel sheets. Since these works, a number of researchers have used the EWF methodology to characterize the fracture properties of several AHSS (DP [10, 45-50], TWIP [46, 51], Q&P [10, 45, 52]) and PHS [45, 53] sheets.

The idea of the essential work of fracture (EWF) was initially proposed by Broberg [54, 55]. He suggested that the ductile fracture process takes place in two different regions: an inner fracture process zone (FPZ, Figure 6) and an outer plastic region. Later, Cotterel and Reddel developed the EWF methodology to experimentally separate these two terms [5]. The work developed in the FPZ is called the essential work of fracture (W_e). It represents the energy necessary to create new surfaces at the front of the crack tip and it is proportional to the fractured area. The work dissipated in the outer plastic zone is the non-essential plastic work (W_p), which depends on the volume of the deformed region around the fracture plane. Then, the total work of ductile fracture can be expressed as follows:

$$W_f = W_e + W_p = w_e\, l_0\, t_0 + w_p\, \beta l_0^2 t_0 \quad (10)$$

where

w_e is the specific work of fracture per unit area;

l_0 is the ligament length;

t_0 is the specimen thickness;

w_p is the specific non-essential plastic work per unit volume;

β is a shape factor that depends on the shape of the plastic zone.

Normalizing Equation (10) by the cross-section area gives:

$$\frac{W_f}{l_o t_o} = w_f = w_e + w_p\, \beta\, l_o \quad (11)$$

Using Equation (11), w_e is determined by testing up to fracture a series of specimens with different ligament lengths (l_o) and plotting w_f values as a function of l_o. w_e and $w_p\beta$ can be obtained by linear regression, where w_e is given by the intercept and $w_p\beta$ by the slope, as shown in Figure 7. w_f values are obtained by integrating the area under load vs displacement curves (W_f) and dividing by the initial cross-section area. It must be noted that w_e cannot be considered as an intrinsic material property since it has an important contribution from necking. Thus, it is a material constant for a given sheet thickness.

Table 4 shows some published w_e values for thin steel sheets.

Table 4 — Reported w_e values for metal sheets

Material	Thickness [mm]	w_e [kJ/m^2]
TRIP steel (8 % austenite vol. fraction) [13]	0,9	270
TRIP steel (24 % austenite vol. fraction) [13]	0,9	50
CP steel 1 000 MPa UTS [45]	1,4	405
DP steel 1 000 MPa UTS [45]	1,4	138
Trip-aided Bainitic Ferritic (TBF) steel [45]	1,4	150
Quenched & Partitioned (Q&P) steel [45]	1,4	194
Press Hardened steel 1 500 MPa [45]	1,5	159
Press Hardened steel 1 000 MPa [45]	1,5	249
Dual Phase 1 000 MPa [50]	1,4	286
Dual Phase 1 000 MPa (6 % retained austenite) [50, 56]	1,4	149
DP 780 (9,8 % retained austenite vol. fraction) [56]	1,5	151
TRIP780 (15,6 % retained austenite vol. fraction) [56]	1,6	106
3rd Gen DP1180 (14,8 % retained austenite vol. fraction) [56]	1,2	115
3rd Gen TBF 1180 (15,5 % retained austenite vol. fraction) [56]	1,4	104

Material	Thickness [mm]	w_e [kJ/m^2]
3rd Gen Q&P 1180 (12,6 % retained austenite vol. fraction) [56]	1,5	196
Q&P steel 1 400 MPa [57]	1,25	40
Dual Phase 752 MPa (equiaxed microstrucute, 19 % martensite vol. fraction) [49]	1,0	214
Dual Phase 854 MPa (equiaxed microstructure, 36 % martensite vol. fraction) [49]	1,0	276
Dual Phase 666 MPa (equiaxed microstrucute, 19 % martensite vol. fraction) [49]	2,0	386
Dual Phase 775 MPa (equiaxed microstructure, 36 % martensite vol. fraction) [49]	2,0	373
Dual Phase 700 MPa (platelet-like microstructure, 19 % martensite vol. fraction) [49]	1,0	345
Dual Phase 741 MPa (platelet-like microstructure, 36 % martensite vol. fraction) [49]	1,0	284
Dual Phase 716 MPa (platelet-like microstructure, 19 % martensite vol. fraction) [49]	2,0	558
Dual Phase 688 MPa (platelet-like microstructure, 36 % martensite vol. fraction) [49]	2,0	595

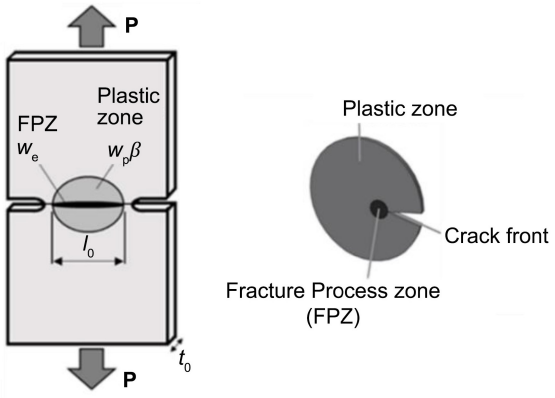

a) b)

Figure 6 — a) DENT specimen used for the evaluation of the EWF [10] and b) definition of the Fracture Process Zone

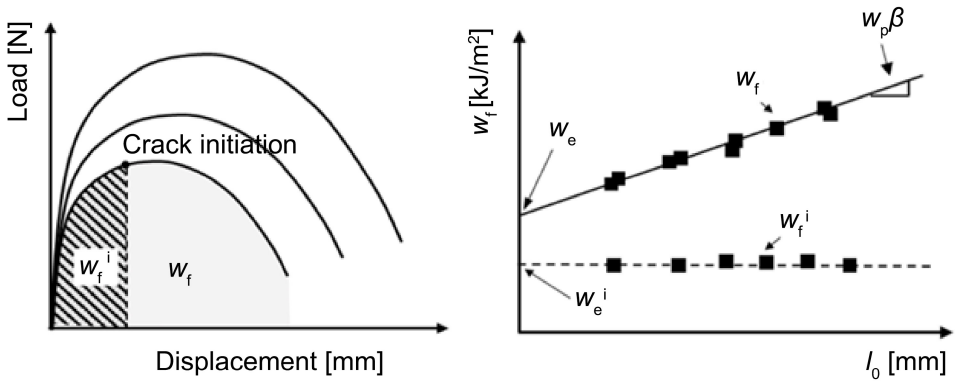

a) **b)**

Figure 7 — Experimental procedure for the determination of the essential work of fracture, w_e and the specific work for fracture initiation, w_e^i [10]. a) Determination of the total work of fracture (W_f) and total work for fracture initiation (W_f^i) from the load-displacement curve, b) specific work of fracture, w_f, and specific work for fracture initiation, w_f^i, as a function of the ligament length, l_0

5.4.1.1 Recommended specimen geometry

w_e has shown to be independent of the specimen geometry and can be obtained from different geometries [29-31]. However, for thin sheets (up to ≈ 3 mm) the recommended specimen geometry is the Double Edge Notched Tension (DENT) specimens (Figure 6) because of its symmetry and minimal specimen rotation and buckling during the test. On the other hand, for thicker plates, the use of DENT specimens involves some extra experimental difficulties. One of the major problems lies in the preparation of the two initial fatigue pre-cracks since, as thickness increases, it is more difficult to obtain similar crack lengths at the two notches of the specimen. If cracks are asymmetric, they do not grow simultaneously during the tensile tests, which increase data scattering and compromise the reliability of the results. Another limitation concerns the high loads required to break the specimens, which makes necessary the use of high-capacity load cells and specimen grips. The use of alternative specimen geometries, such as the Single Edge Notched Bending (SENB), can simplify considerably the specimen preparation and testing (Figure 8). The SENB geometry has been used to characterize the EWF of ductile polymers with similar results to those obtained with DENT specimens [29]. In the *FormPlanet* project, SENB specimens were successfully used to characterize the EWF of thick 22MnB5 steel plates with different heat treatments. The results were very helpful to understand the role of microstructure on the crack propagation resistance of thick high strength steels (Figure 9).

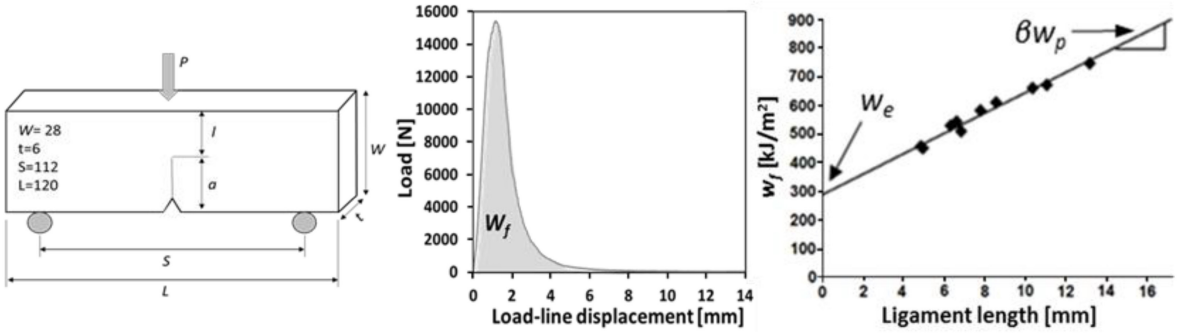

Figure 8 — Experimental procedure for the determination of the essential work of fracture using SENB specimens

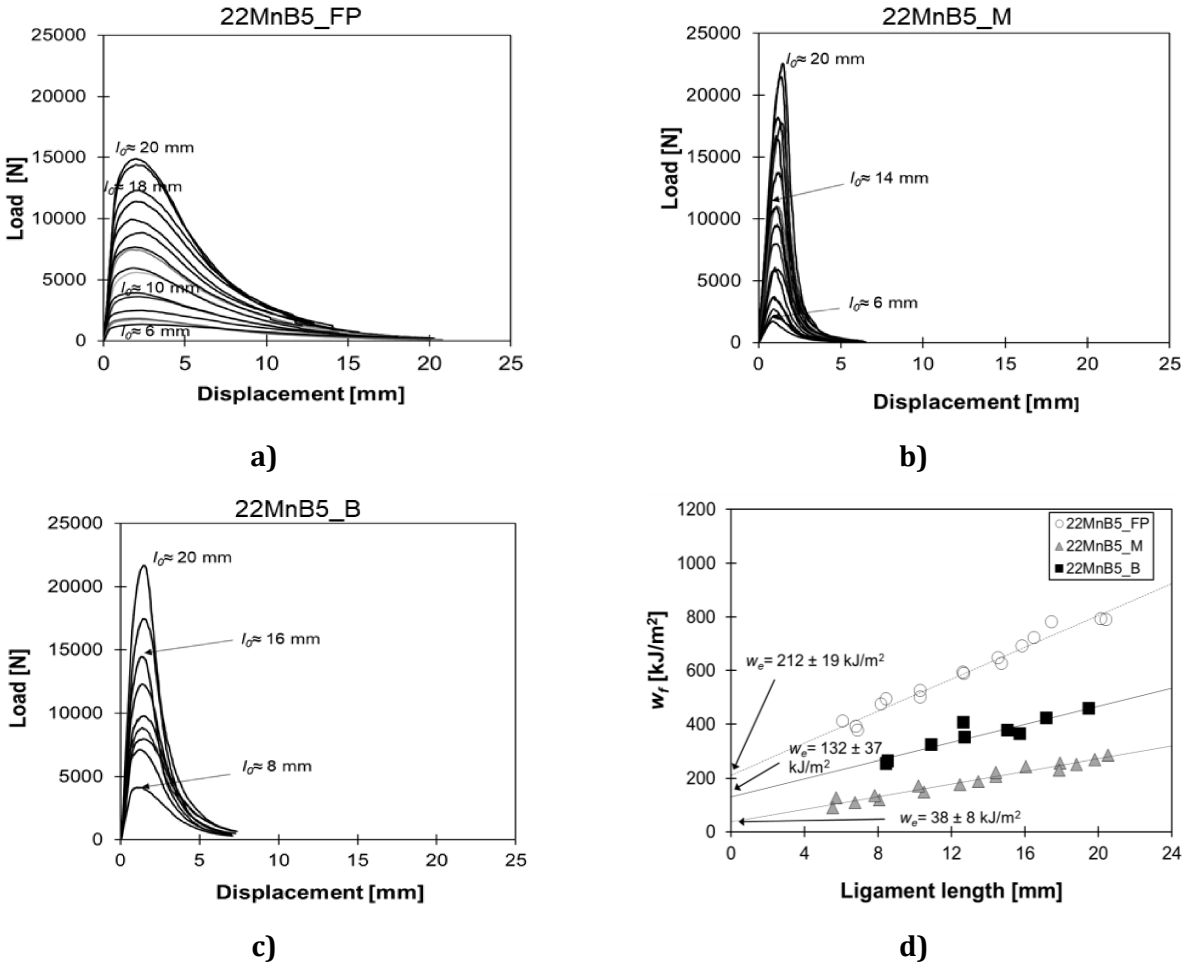

Figure 9 — Load vs load-line displacement curves from EWF tests with SENB specimens for thick 22MnB5 steel sheets at different conditions: a) As-received state (Ferrite-Pearlite), b) Fully hardened (Martensite), c) Controlled Cooling (Bainite), d) w_f as a function of the ligament length for the different thick 22MnB2 steel sheets

5.4.1.2 Selection of ligament length range and specimen dimensions

The EWF must be extracted by linear regression over a series of tests with varying ligament lengths. The simplest procedure consists in testing an arbitrary number of samples with a defined height and width and ligament lengths spread equidistantly over the range of ligament lengths satisfying the validity criteria of the EWF method, with each test repeated at least once to observe the variance of the experiments. This straightforward method can become a hindrance when the quantity of available material is limited and/or expensive.

Adapting the tensile specimen geometry to the ligament length is an effective approach to reduce the total material used. Indeed, a test is valid if the ligament is fully yielded before crack propagation, and if the plastic zone is confined to the ligament. The first condition depends only on the ligament length and the material. The second condition depends on the ligament length, the material, and the width of the specimen, in the case of the double edge notched geometry. In other words, as long as the sides of the specimens do not interact with the plastic zone, the width and height of the specimen can be reduced. In practice, this translates to a width that can be reduced to twice the ligament length and a height that is twice the width. It is worth noting that the minimum height will also need to consider the size of the specimen holding mechanism (clamping jaws, pins, etc). Figure 10 [58] shows a comparison between three sets of specimens of the same material. The first set (in blue) uses full size specimens, the second set adapts the specimen height and width to the ligament lengths, the third set has identical height but varying width for a ligament length of approx. 10 mm. The extracted EWF between the first two set are in very good agreement. The third set shows that these new data points are not statistically different from the other two data sets and could be part of the same regression. This confirms that adapting the specimen geometry to the ligament length does not negatively impact the extraction of the EWF by linear regression.

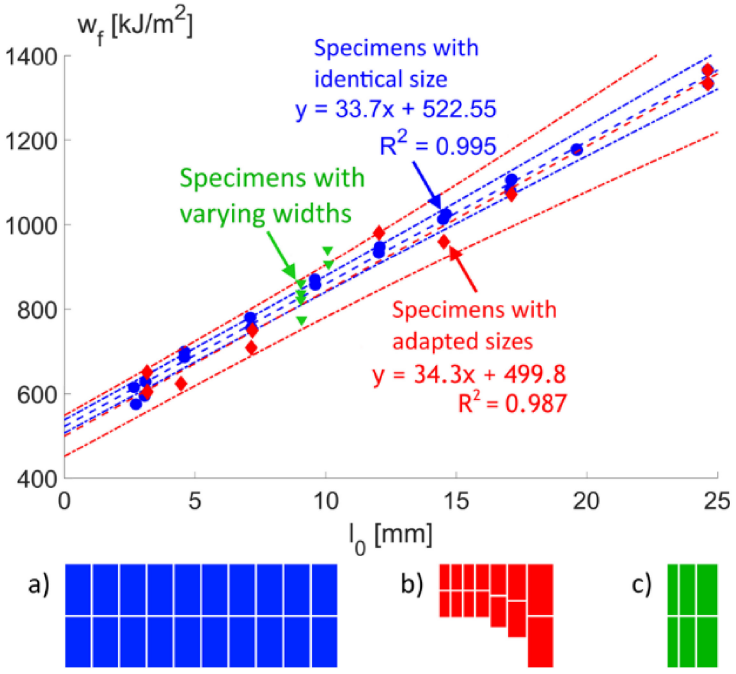

Figure 10 — Comparison of the EWF methodologies using standard DENT specimens with identical size of 50 mm x 100 mm (blue circles) and using reduced and adapted specimen sizes (red diamonds) as a function of the ligament length. Ordinary least-squares linear regressions are presented as dashed lines. Confidence intervals are shown by dotted lines. Specimens with similar ligament length and identical height of 100 mm but with varying width of 20 mm to 40 mm are represented with green triangles. The specimens dimensions are schematically represented with identical sizes in a), adapted sizes in b), and with varying width in c). [58]

The second method to reduce the quantity of required material is based on the observation that testing a specimen with a ligament length close to the lower ligament length bound has a stronger impact to the linear regression than any other length. By optimizing the distribution of ligament lengths, a smaller number of specimens can be tested while conserving the same statistical error on the extracted EWF. Similarly, the same number of specimens can be tested while improving the accuracy of the EWF method.

Combining this strategy with a geometry adapted to the specimen size can tremendously reduce the total amount of material. For example, assuming a lower and upper ligament length bounds of 5 mm and 25 mm, respectively, and DENT specimens with the width equal to twice the ligament length and the height equal to twice the width, a 80% reduction of material can theoretically be achieved [58]. This approach is based on a rigorous statistical model validated numerically and experimentally [58]. The model allows to investigate different scenarios. In order to minimize the amount of material, one should test specimens with ligament lengths at the boundaries of the valid range, λ_min and λ_max. The proportion of specimens with a ligament length of λ_min, the lower ligament length bound, should be equal to p_(λ_min)=1/2+√6/6≈0,91. The proportion of specimens with a ligament length of λ_max, the upper ligament length bound, should be equal to p_ (λ_max)=1/2-√6/6≈0,09. In order to minimize the error on the EWF, one should test specimens with ligament lengths at the boundaries of the valid range as well. The proportion of specimens with a ligament length of λ_min should be equal to p_(λ_min)=λ_max/(λ_min+λ_max). The proportion of specimens with a ligament length of λ_max should be equal to p_(λ_max)=λ_min/(λ_min+λ_max).

5.4.1.3 Recommended crack preparation procedure

In order to replicate a real crack propagation during an EWF test, a pre-crack should be realized. The crack tip diameter (δ_0) of this pre-crack should be smaller the CTOD at crack initiation (δ_c) of the tested material. An experimental method for determining the CTOD at crack initiation can be found in [59] and is resumed hereafter.

In [59], a method is proposed for measuring the Crack Tip Opening Displacement (CTOD) at physical cracking initiation in ductile materials. The method requires a few pre-cracked specimens to be loaded at different levels in order to involve various crack extensions. The total opening of the blunted pre-crack, δ_1, the opening of the tearing crack, δ_2, and the ductile tearing extension are measured for each specimen. The unloaded CTOD at cracking initiation is equal to the difference δ_1 - δ_2 extrapolated to zero crack extension. This mechanism is illustrated in Figure 11.

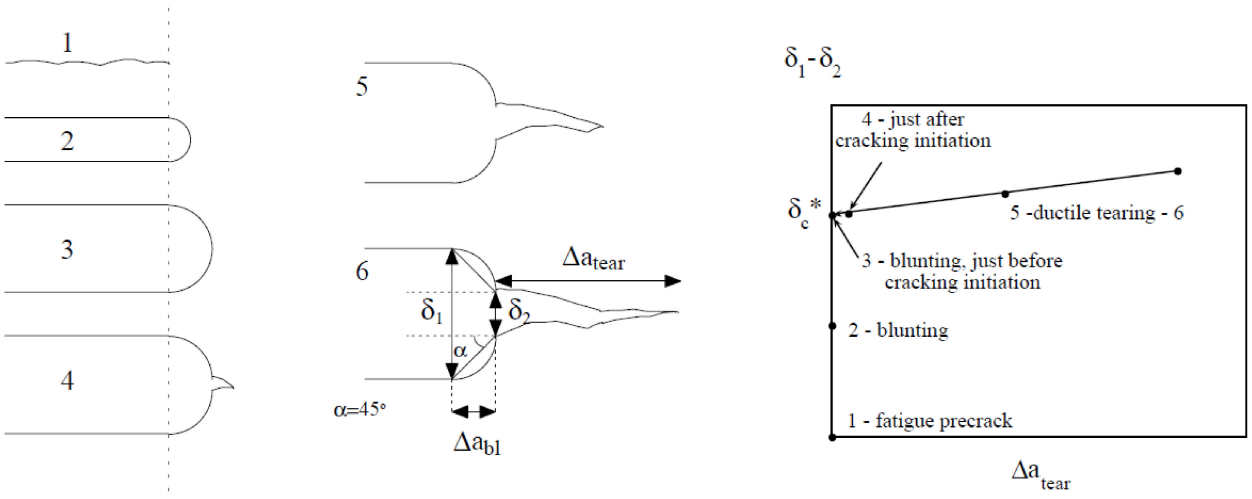

Figure 11 — Crack blunting before propagation mechanism in a ductile material [59]

In order to pre-crack the EWF specimen, the crack tip radius should be less than one sixth of δ_c with a pre-crack length of at least δ_c.

Depending on the crack tip radius needed to be achieved, several methods to pre-crack the specimen are available. Except for the punching method developed by Eurecat and describe below, all methods require the sample to be notched; ideally with EDM (electro-discharge machining) giving a notch radius of around 150 µm as illustrated in Figure 12 a. The most recommended method for crack preparation is the fatigue pre-crack from a notched specimen as it results in a crack tip radius of around 0,1 µm. The major downside of this method is the time required for the preparation (around 1 h per specimen).

Another method is to pre-crack the notched specimen with a thin razor blade with a sawing motion for several minutes, actual time will depend on the material and the thickness of the specimen. The crack tip radius achieved with this method is around 50 µm. A pre-crack realized with this method is illustrated in Figure 12b.

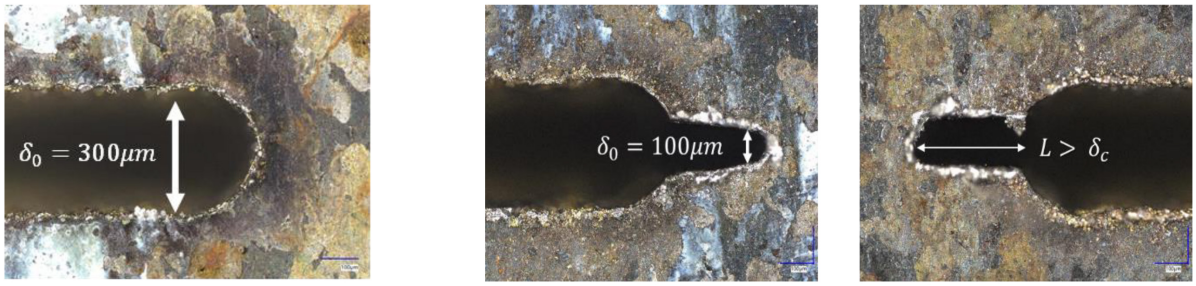

a) **b)**

Figure 12 — a) EDM pre-cracking, b) pre-cracking with a razor blade

Lastly, Eurecat has developed a tool to avoid fatigue pre-cracking of specimens. The tool permits to easily introduce sharp notches (notch radius similar to fatigue pre-crack) in metallic sheets with a simple shearing process. The device, described in detail in [60], consists of a two-pillar modular cutting die, equipped with a bevelled punch (Figure 13 a) designed to introduce crack-like sharp notches in thin sheet specimens (up to 4 mm thickness). The tool allows obtaining rectangular Double Edge Notched Tension (DENT) specimens (Figure 13 b) by means of a simple shearing process.

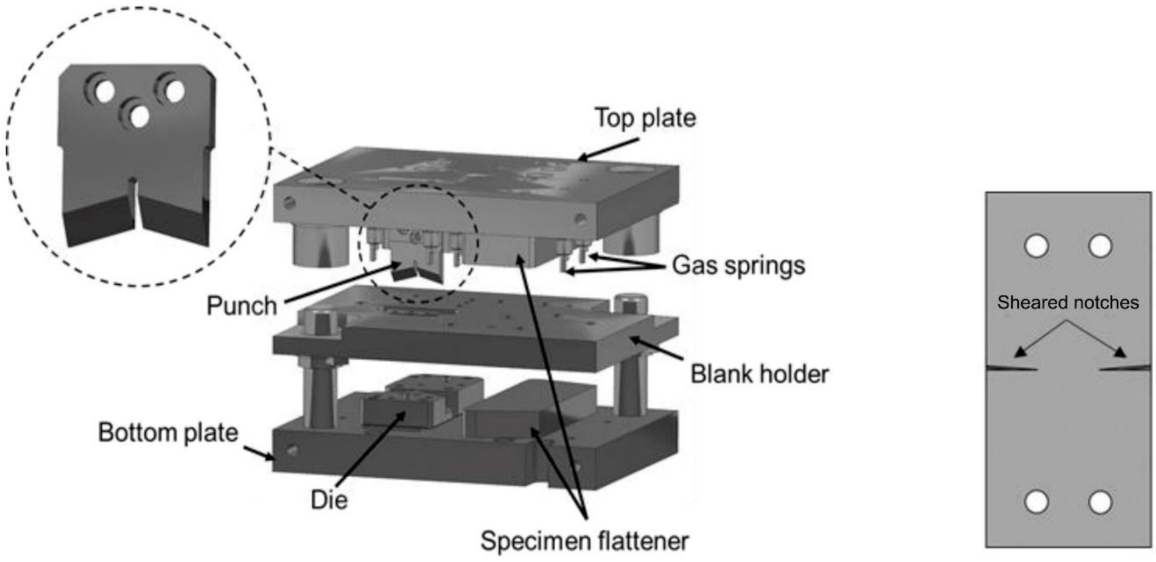

Figure 13 — a) Tool for introducing sharp notches in sheet metal specimens and detail of the bevelled punch. b) DENT specimen with sheared sharp notches [60]

An example of the experimental setup of the notching tool in a testing machine is illustrated in Figure 14. The experimental procedure for specimen notching is schematized in Figure 15. The process is described as follows: first, a rectangular specimen of 200 mm × 55 mm (cut at transverse orientation with respect to the rolling direction) is placed at the die and fixed using 2 pins (Figure 14 c). This fixation system ensures the alignment of the specimen and that notches are always centred with respect to the pinning holes. Then, the punch is moved downwards and, by means of a shearing process, two sharp notches (notch radius, $\rho \approx 2\text{-}3$ μm) are introduced in the specimen (notches symmetrical with respect to the longitudinal axis of the specimen). The ligament length is modified by controlling the punch displacement, i.e. the greater the punch displacement the smaller the ligament between the two notches. After cutting, the punch returns to the initial position and the specimen can be extracted and tested.

The new rapid notching procedure has been validated in a wide range of AHSS sheets providing equivalent EWF results to those obtained with fatigue pre-cracked specimens (Figure 16). The new methodology supposes great time savings and it might be implemented as a routine procedure for in-plant quality control and material selection and/or acceptance.

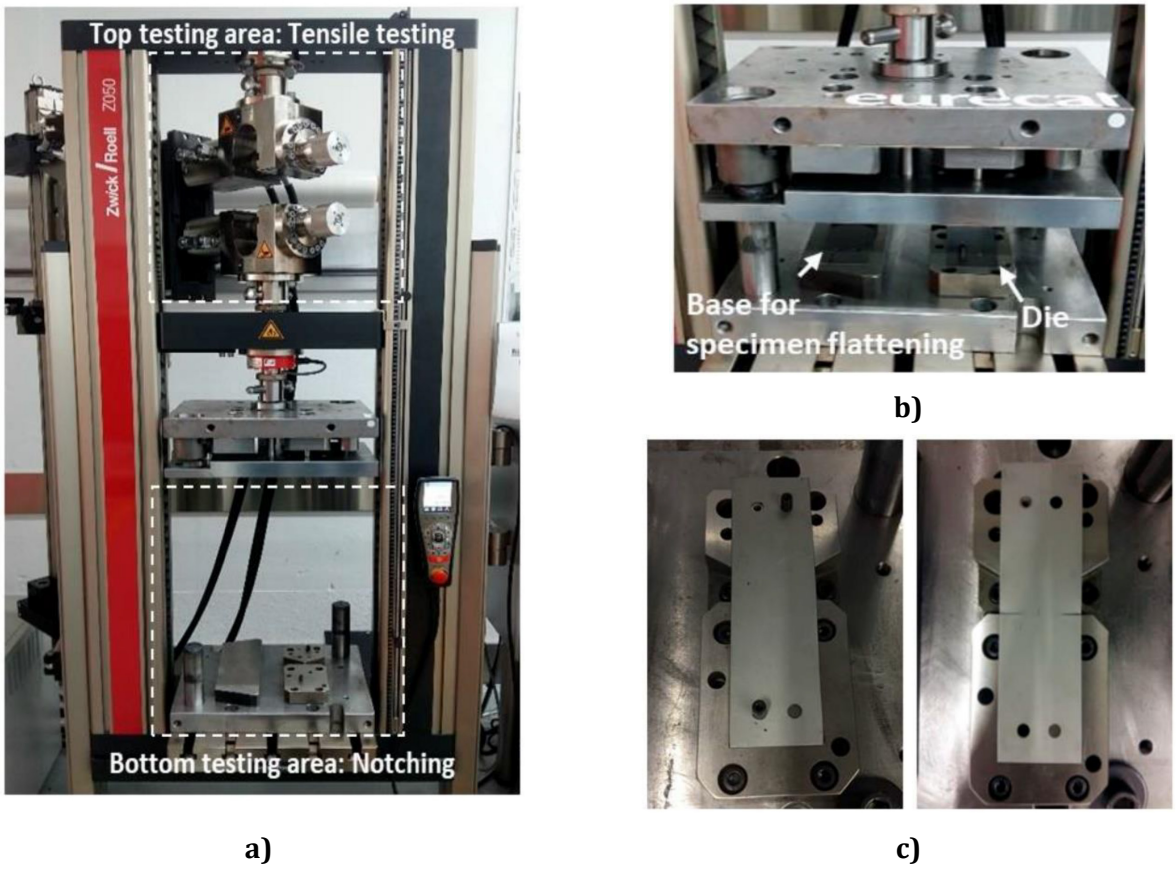

Figure 14 — Images of the experimental setup for the notching process. a) Setup of the tool in the testing machine. b) Detail of the cutting tool. c) Specimen before (left) and after (right) the notching process [60]

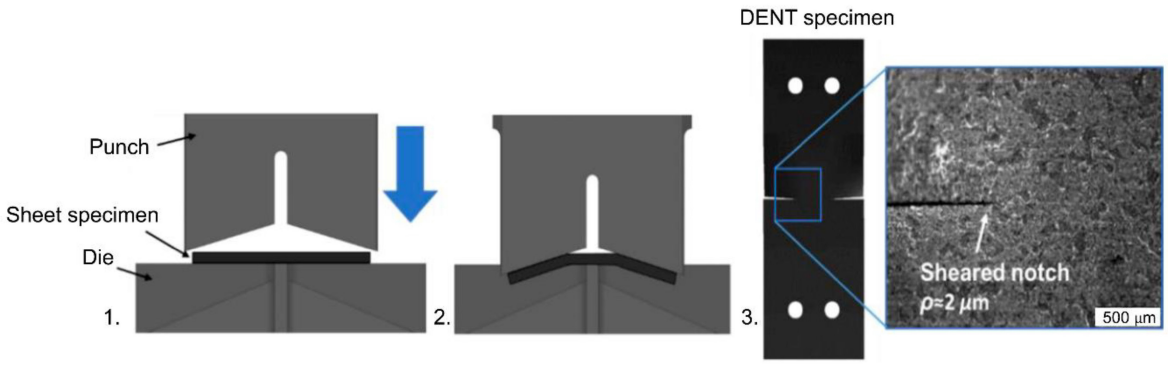

Figure 15 — Schematic representation of the experimental procedure for the preparation of sheared notches in sheet specimens [60]

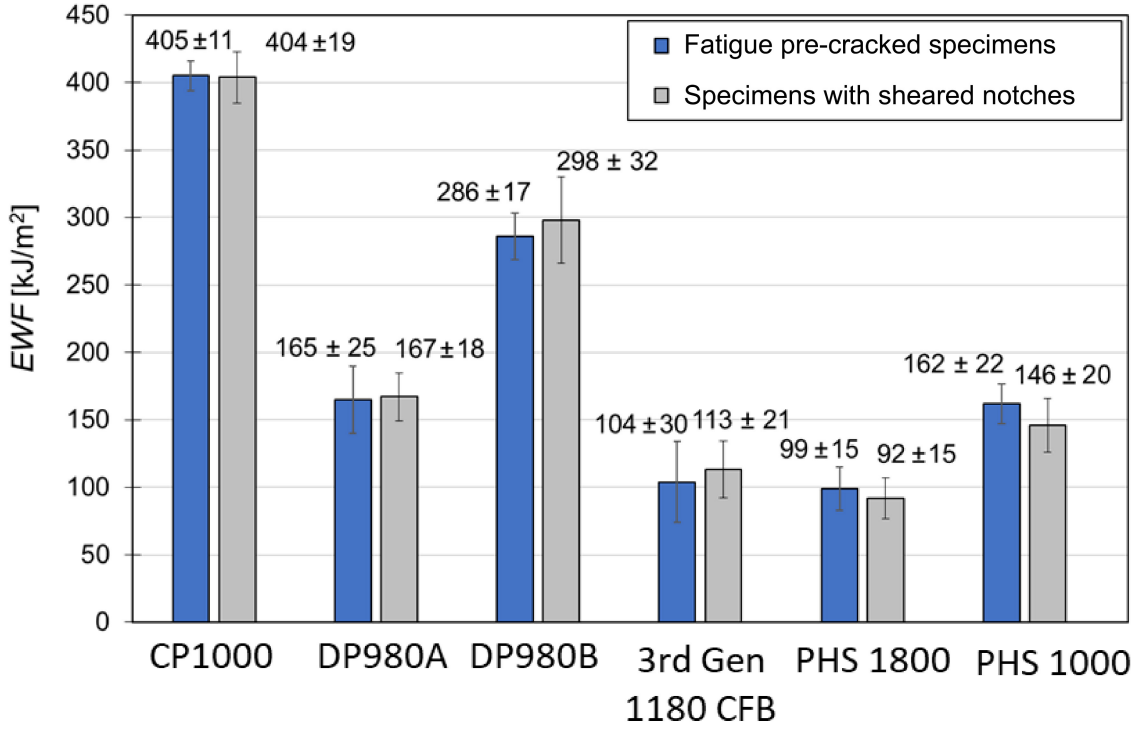

Figure 16 — w_e values obtained from EWF tests fatigue pre-cracked (blue) and sheared (grey) specimens. Results from FormPlanet project

5.4.1.4 Recommendations for linear regression analysis

The EWF method is based on linear regression. The accuracy and confidence of the extracted EWF can be improved and discussed by rigorous statistical analysis. Three approaches are proposed in this section which have been experimentally validated:

1. Studentized residual analysis:

Residuals can give a deep insight on the overall validity of the linear regression and can also help spot outliers [58]. Residuals are usually defined as $r = y_f - y$, where y_f are the measured values and y are the model values. However, it is possible to normalize the residuals in such a way that they follow a Student distribution. This allows to define outliers in terms of a p-value, e.g. outliers fall outside the range of [-1,96, 1,96] for a p-value of 0,05. The studentized residuals are given by

$$r_{stud} = \frac{r}{\sqrt{\frac{SSR}{n-2}\left(1-\left(\frac{1}{n}+\frac{\left(y_f-\bar{y}\right)^2}{\sum_{i=1}^{n}\left(y_{f_i}-\bar{y}\right)^2}\right)\right)}} \tag{12}$$

Moreover, the Studentized residuals should be normally distributed around 0, otherwise, it might indicate that a linear regression model is not a good choice.

2. Confidence intervals and error estimation on the extracted EWF

The confidence intervals (CI) represent the interval containing the true line (i.e. the true behaviour) with a probability of 100 – α%. The intervals give a visual representation of the potential error on the slope and intercept of the regression. The CI are defined as

$$CI = \widehat{\beta_0} \pm t(1-\alpha/2, n-2)\, se(\widehat{\beta_0}\,|\,x) + \left(\widehat{\beta_1} \pm t(1-\alpha/2, n-2)\, se(\widehat{\beta_1}\,|\,x)\right)x, \tag{13}$$

where

$$se(\widehat{\beta_0}\,|\,x) = \sqrt{\sigma^2\left(\frac{1}{n} + \frac{(x-\bar{x})^2}{\sum(x_i-\bar{x})^2}\right)}, \tag{14}$$

$$se(\widehat{\beta_1}\,|\,x) = \sqrt{\sigma^2\frac{1}{\sum(x_i-\bar{x})^2}}, \tag{15}$$

The error on the EWF with a given p-value can be computed using the CI at $x = 0$.

3. Linearity test

A linearity test (Chow's statistical test) evaluates if two datasets can be represented by the same linear regression [39]. In the case of the EWF method, Chow's test can be used to identify outliers as well as to identify a loss of linearity, e.g. to identify λ_{min} and λ_{max}. The test consists in evaluating $F_{obs} = \frac{(n-2)(SSR^* - SSR)}{SSR}$, following a Fisher distribution.

5.4.1.5 Crack initiation and propagation resistance, $w_e{}^i$ and w_e

The specific essential work of fracture, w_e, is obtained from an average of w_f values for the complete fracture resistance and, therefore, it contains energetic contributions from both crack initiation and propagation resistance. Mai and Cotterell [30] showed that the EWF methodology also permits to separate from both contributions and determine a fracture toughness value for crack initiation. As shown in Figure 7, for each ligament length the work of fracture at crack initiation ($w_f{}^i$) can be obtained by integrating the area under the load-displacement curve up to the point of crack growth initiation. Since $w_f{}^i$ is independent of the ligament length [10, 30], a specific essential work for fracture initiation, $w_e{}^i$ can be calculated from an average of $w_f{}^i$ values. Usually, $w_e{}^i$ is lower than w_e, however, the differences between w_e and $w_e{}^i$ can significantly vary from one material to another. This is illustrated in Figure 17, where $w_e{}^i$ and w_e values for a wide range of AHSS and PHS are plotted. In steels with a small contribution from crack propagation resistance after initiation ($w_e{}^i \approx w_e$), a single initiation toughness value can be representative of the material's fracture toughness. However, in steels showing an important contribution from crack propagation resistance ($w_e >> w_e{}^i$), initiation toughness can completely underestimate the overall crack propagation resistance of the material.

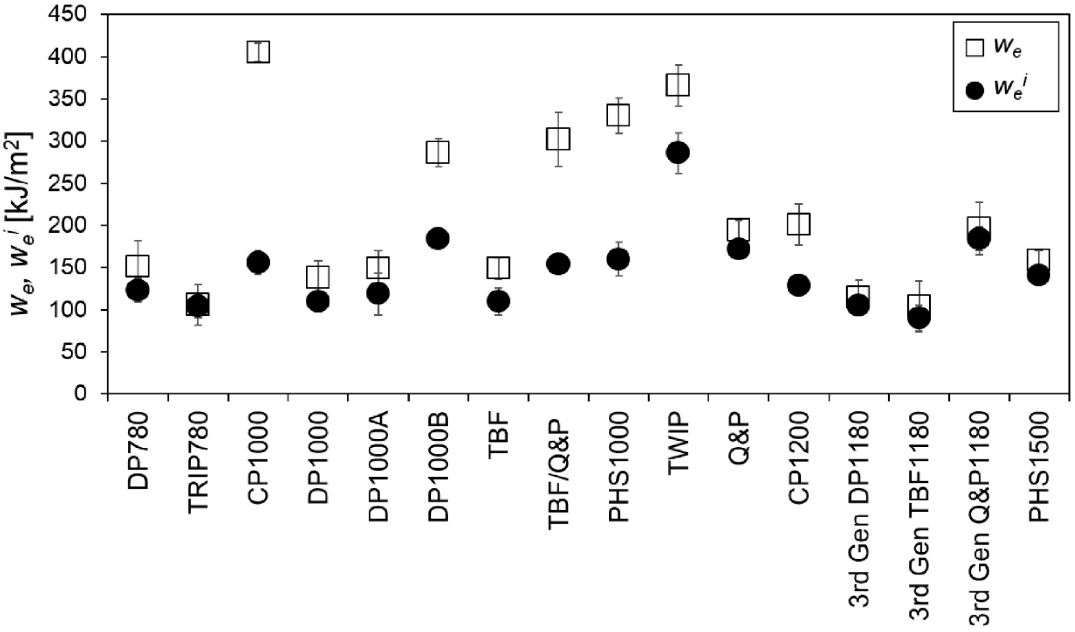

Figure 17 — w_e and $w_e{}^i$ values for different AHSS and PHS steels [61]

5.4.1.6 EWF standardization

Despite the important potential of the EWF method to readily measure the fracture resistance of thin ductile sheets under plane stress conditions, no standard procedure has been developed yet. One of the main challenges in EWF standardisation is the sensitivity of the method to different testing variables: notch quality (sharpness, alignment), number of specimens, ligament length range, etc. Different attempts have been made to standardise the EWF methodology [62-65]. Nowadays, the most extended procedure for the evaluation of the EWF is the testing protocol developed by the European Structural Integrity Society (ESIS) TC4 committee (TC04- Polymers, Polymer composites and adhesives) [62]. This protocol is based on a series of round-robin tests during a seven-year period, with the participation of 23 laboratories. The protocol provides the guidelines for the evaluation of the EWF by using DENT specimens and discuss some of the most critical points related to specimen preparation, testing and data analysis.

However, this protocol is focused on the fracture testing of polymers and composites. Therefore, no recommendations are given about the notch preparation in metallic materials. To fill the lack of standard methods for EWF testing of metal sheets, a CEN Workshop Agreement (CWA 17793:2021 Test method for determination of the EWF of thin ductile metallic sheets) [66] has been developed very recently in the frame of the H2020 project *FormPlanet*. This reference document includes recommendations about specimen geometry, testing and data processing. It also contains different validation criteria to ensure the validity of the EWF methodology and describes a novel notching procedure to drastically reduce the time of specimen preparation (see more details in 5.4.1.3).

5.5 Summary of fracture toughness testing methods

The main experimental methods to characterize the fracture toughness of thin ductile metal sheets described in the previous section are summarized in Table 5. The table indicates the standard document that describes the experimental procedure, the main fracture parameters obtained, and a classification index based on the experimental complexity of each method. The index is defined on a scale of 1 to 4: 1 – Very simple, 2 – Simple, 3 – Complex, 4 – Very complex. The level of complexity is defined according to the difficulty of specimen preparation, the need for special equipment (fatigue machines, digital image correlation, microscope, etc.), the complexity of the test itself (continuous crack growth monitoring, indirect crack growth measurements, etc.) and the amount of data post-processing.

Among the different testing methods described, the EWF is the most recommendable procedure to evaluate the crack initiation and propagation resistance of high strength metal sheets due to its relative simplicity and usefulness to understand the fracture behaviour of these materials. Additionally, with the new rapid notching procedure described in 5.4.1.3, the methodology is much simpler and can be easily used as a rapid test method for materials screening or quality control of raw materials.

According to this, the following sections are focused on the application of the EWF method at different stages of AHSS manufacturing, from the microstructural design to the industrial implementation of high-performance sheet metal products.

Table 5 — Summary of fracture toughness testing methods and fracture parameters

Method	Standard	Fracture parameters	Definition	Complexity
***J*-integral**	ASTM E1820 / ISO 12135	J_{ic} / $J_{0,2BL}$, *J-R* curve	— J_{ic} / $J_{0,2BL}$ *J*-integral near the onset of stable crack propagation — *J-R* , *J*-resistance curve, *J* values as a function of the crack extension	4
CTOD	ASTM E1820 / ISO 12135	δ_{Ic} / $\delta_{J0,2BL}$	Critical crack tip opening displacement	4
CTOA	ASTM E2472 / ISO 22889	ψ_c	Critical crack tip opening angle	3
δ_5	ASTM E2472 / ISO 22889	δ_5	Crack opening displacement over a 5 mm gauge length at tip of fatigue pre-crack	3
Kahn Tear Test	ASTM B871 (Withdrawn 2017)	*UIE*, *UPE*	— *UIE*, Unit Initiation energy — *UPE*, Unit Propagation Energy	1
Essential Work of Fracture	CWA 17793:2021	w_e^i, w_e	— w_e^i, specific essential work of fracture initiation — w_e, specific essential work of fracture	2

6 Fracture toughness: a key material property for material design

6.1 Fracture toughness in engineering materials design

Fracture toughness is considered as a key design parameter for engineering applications where structural integrity is of primary importance, such as pipelines in oil and gas industries, nuclear plants, pressure vessels, aeronautics, etc. However, until the rise of AHSS, fracture toughness has not been considered to be relevant to automotive designers mainly due to the large ductility of conventional mild steels. Moreover, the complexity of fracture mechanics testing and the absence of affordable standard procedures for fracture toughness characterization of thin metal sheets have generated a gap of knowledge in this field. Nevertheless, due to the increasingly demanding performance requirements and the frequent occurrence of failures related to the crack initiation and propagation resistance in AHSS, the knowledge on the fracture toughness properties of high strength metal sheets has become unavoidable.

6.1.1 Microstructural optimization

Traditionally, the microstructure of high strength metal sheets has been optimized according to strength and elongation properties from tensile tests, while limited attention has been paid to their crack propagation resistance. When referring to toughness, the product of the ultimate tensile strength (UTS) by the total elongation (TE) has been often used in literature. This parameter represents a combination of the material's strength and ductility and is conventionally used as a performance index of AHSS [67]. The common perception is that a higher UTS × TE product implies higher fracture toughness. However, as proven by different authors [13, 56, 61, 68] and illustrated in Figure 18, no clear link can be established between crack propagation resistance and this parameter. Other parameters, such as the true fracture strain (TFS) derived from the area reduction at fracture in tensile tests or the True Thickness Strain (TTS) are also increasingly used as a measure of fracture resistance and local formability of AHSS [67, 69]. These local strain measurements may provide a better estimation of fracture toughness (Figure 18). Nevertheless, as shown by Xiong et al. [68], these fracture-related parameters are not accurate enough to describe the fracture behaviour of high strength sheet materials in the presence of existing cracks or defects. Therefore, to better understand the fracture performance of AHSS sheets, including crack initiation and propagation resistance, fracture toughness should be properly measured in the frame of fracture mechanics.

Fracture toughness is very sensitive to the material's microstructure and can therefore be used as a very useful tool for microstructural optimization in terms of fracture resistance and damage tolerance. For example, concerning AHSS microstructures, it has been shown that Complex Phase (CP)-like microstructures, which consist of a homogeneous bainite/tempered martensite matrix with small amounts of secondary phases in different proportions (martensite, ferrite, austenite), present higher fracture toughness than Dual Phase (DP)-like ones (soft ferrite/bainitic ferrite matrix with the presence of hard martensite) [45, 70, 71]. However, as discussed in [50], DP microstructures can also be designed to attain comparable fracture toughness to CP steels showing similar strength but at the expense of global ductility (strain hardening and elongation). Ismail et al. [49] demonstrated the important role of martensite morphology on the fracture toughness of DP steels and how microstructural design can be used to obtain optimized microstructures with improved fracture properties.

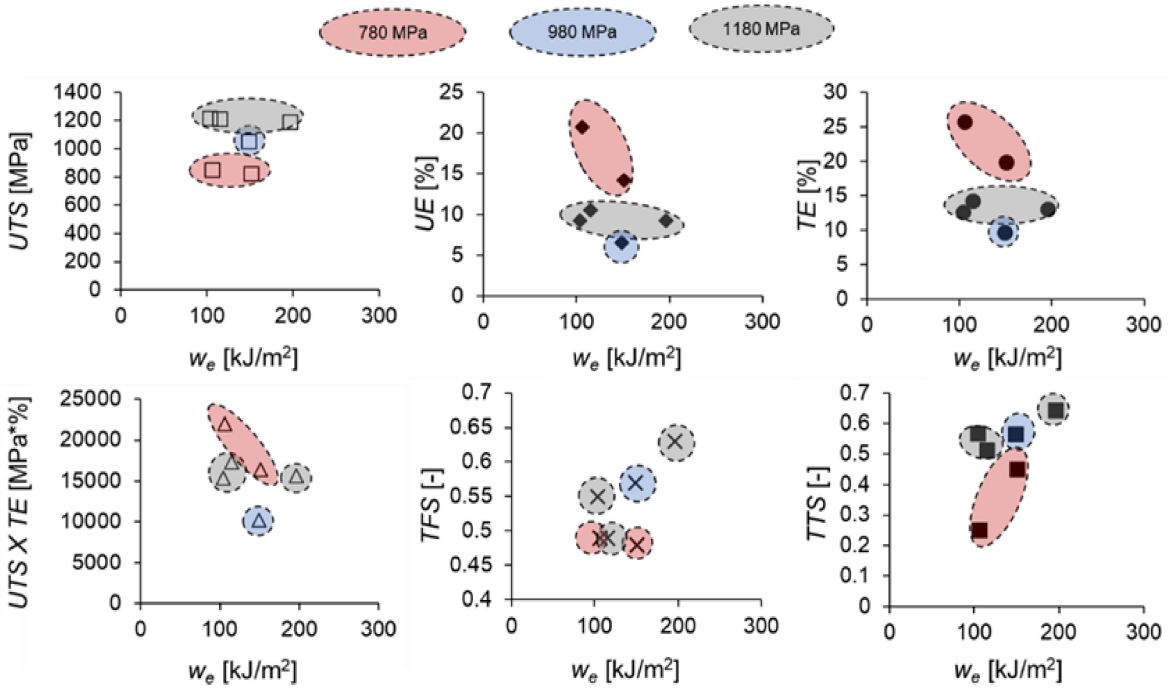

Figure 18 — Correlation between fracture toughness and uniaxial tensile properties for different AHSS [56]

A wide range of opportunities is opened in the design of AHSS microstructures with the emergence of 3rd Generation AHSS. In this context, fracture toughness could be even more important than for other steel families. 3rd Gen AHSS rely on the strain-induced retained austenite (RA) to martensite transformation, also known as Transformation-Induced Plasticity (TRIP) effect, which contributes to improving ductility and strength. The beneficial influence of the TRIP effect on mechanical properties is associated with the formation of additional geometrically necessary dislocations during the strain-induced martensitic transformation, which increases work hardening and delays the onset of necking [72, 73]. The amount of generated dislocations depends on the amount of the RA transformed. Therefore, a higher RA volume fraction implies a higher contribution of the TRIP effect to the mechanical performance (Figure 19). Nevertheless, RA may have a detrimental effect on crack propagation resistance [13, 56,57]. This detrimental effect of RA on cracking resistance is attributed to the higher stress triaxiality present in the crack tip which significantly increases the RA to martensite transformation rate. Consequently, the brittle network of fresh martensite created in the fracture process zone favours damage and rapid crack propagation [68, 72]. Different studies have revealed that other factors, such as the RA morphology, size or stability also affect the fracture resistance of TRIP-assisted steels [13, 68, 72]. Therefore, to obtain an optimum balance between fracture resistance and global formability, the RA volume fraction and stability as well as the morphology and matrix characteristics, should be carefully controlled. These findings highlight the importance of fracture toughness measurements on the microstructural design of high-performance sheet metals.

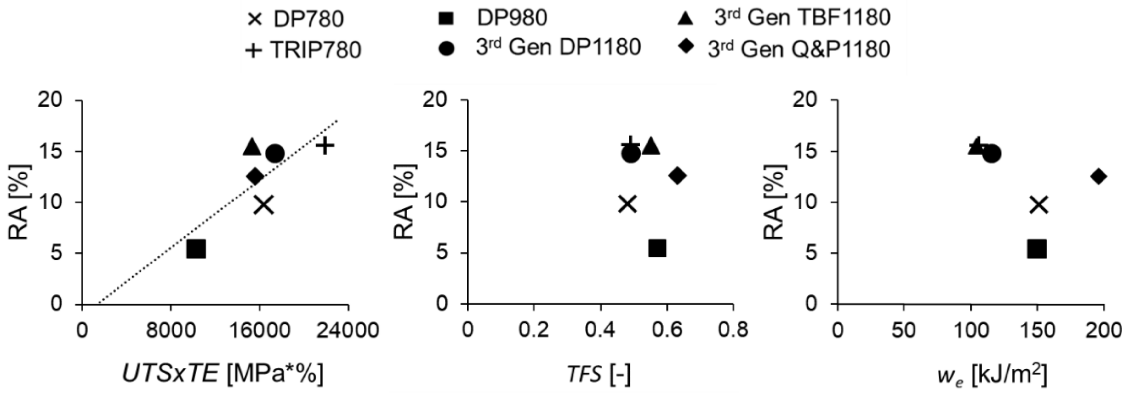

Figure 19 — Relation of RA content with strength/ductility and fracture resistance parameters [56]

7 Fracture toughness measurements for material selection

7.1 Fracture toughness to select materials with improved cracking resistance

Several research studies have evidenced that fracture toughness is a useful property to rationalize and predict cracking-related phenomena in AHSS sheets, such as edge fractures, crash failure or local formability issues [28, 45, 71, 74, 75]. For instance, the good correlation between the specific essential work of fracture (w_e) and the Hole Expansion Ratio (HER) shown in Figure 20 indicates that edge fracture resistance is closely related to crack propagation resistance. This is an important observation when considering the most adequate parameters to estimate the cracking behaviour of AHSS, since crack initiation parameters (w_e^i, UIE, J_c) may underestimate the full fracture performance of some steel grades with significant crack propagation resistance after initiation [10]. As mentioned before, other parameters related to the crack propagation energy, such as UPE from Kahn Tear Tests, also may provide wrong toughness rankings and are not suitable either to accurately estimate crack propagation resistance (Figure 21).

Compared to the HER, w_e provides a more objective and accurate description of the material's fracture resistance. Although the fracture mechanisms involved in both hole expansion tests and fracture mechanics tests are similar [56], strictly speaking, the HER is not a material parameter since it depends on several experimental factors such as the hole preparation method (cutting/punching clearance, cutting tool condition, etc.), the geometry of the expansion tool and the method used for crack detection, among others. All these experimental artefacts increase the scattering of results and lead to poor repeatability, compromising thus the reliability of the HER [76, 77]. On the other hand, w_e is a (thickness dependent) property that represents more accurately the crack propagation resistance of AHSSs and allows to better understand different fracture phenomena related to the damage tolerance and cracking resistance, such as edge fracture.

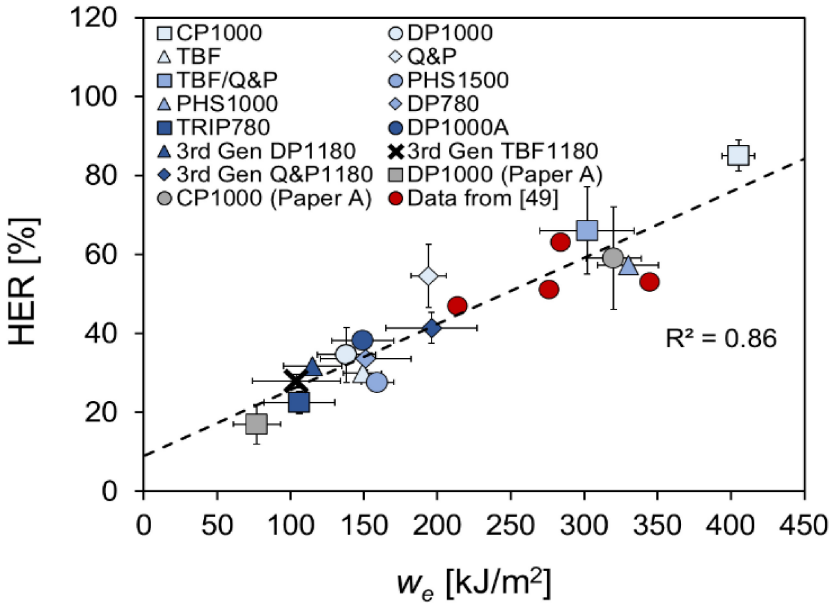

Figure 20 — Correlation between w_e and HER [49, 56, 61]

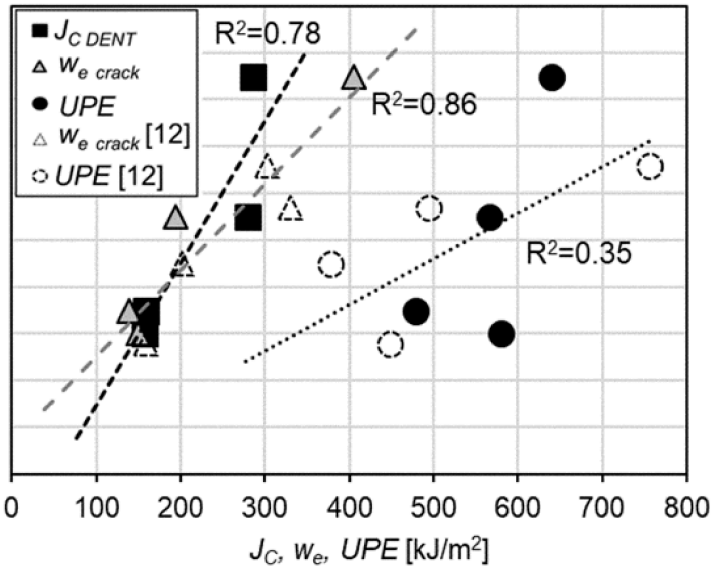

Figure 21 — Correlation between HER and fracture toughness parameters (J_C, w_e and UPE) [10]

Similar observations have been made about the relationship between fracture toughness and the fracture behaviour of AHSS under impact loading [71]. The crash behaviour of very high strength steels is strongly affected by the nucleation and propagation of cracks [71, 78-84]. Accordingly, some authors have proposed the evaluation of their performance according to their cracking behaviour in crash tests. This approach was firstly proposed by Walp in 2007 [79]. Walp described a crack rating index (RVI) to define the impact performance of high strength steels. This index was based on visual evaluation of cracking in tested samples and the determination of an average crack length. He defined three performance levels based on the average crack length (RVI 15-20: Average crack length < 10 mm, RVI 10-25: Average crack length 10-25 mm, RVI 0-9: Average crack length < 25 mm). Later, Larour et al. adapted this methodology and developed the crash index (CI, Table 6), which has been applied to assess the crash behaviour of

several AHSS and PHS grades [80-82, 84]. A similar approach based on a total crack length in crash-tested specimens was used by Link et al. [83] to classify the crash performance of AHSS.

Table 6 — Definition of Crash Index [80]

Crash Index (CI)	Damage
100	No cracks
> 75	Crack length < 10 mm
50-75	10 mm< crack length < 25 mm
25-50	Crack length > 25 mm
< 25	"Splitting and curling", multiple breaks

From these observations, and knowing the influence of crack propagation resistance on crash performance of AHSS, it is reasonable to think that crash resistance might be rationalized in terms of the property that quantifies the material's crack propagation resistance, i.e. the fracture toughness. Larour et al. [81] suggested that the overall crash failure behaviour of AHSS and PHS was mainly dominated by the bendability (resistance to crack initiation) and the fracture toughness (how rapid these cracks propagate through the material). Frómeta et al. [71] investigated the correlation between the axial crash performance of several AHSS and their fracture toughness, measured by means of the essential work of fracture methodology. They evaluated the crash performance according to an overall cracking appearance, measuring the cracks in tested specimens (Figure 22) and using the *CI* described in Table 6, and the maximum energy absorption capacity of the steels. An additional parameter was also introduced, the Crash Index Decreasing Rate (*CIDR*), which defines how rapid the *CI* decreases with the intrusion level. The term intrusion refers to the plastic deformation of crash-tested samples determined by the difference in length between unloaded and crashed samples. The *CIDR* quantifies the crack propagation rate in crash-tested samples, i.e. a high *CIDR* indicates that the *CI* rapidly decreases with the intrusion level and, thus, that cracks rapidly propagate through the sample. This is translated into poorer crash foldability and overall fracture performance. On the other hand, a low *CIDR* means that the material has a higher resistance to crack propagation with increasing intrusion level. As shown in Figure 23, a good correlation was obtained between essential work of fracture measurements and crash performance parameters. The results also showed that, as mentioned above, crack initiation resistance (w_e^i) is not suitable enough to estimate the overall cracking behaviour of AHSS during axial crash tests.

All these results highlight the relevant role of fracture toughness on the edge cracking and crash resistance of AHSS and pose w_e as a key property for the selection of AHSS grades with enhanced fracture resistance.

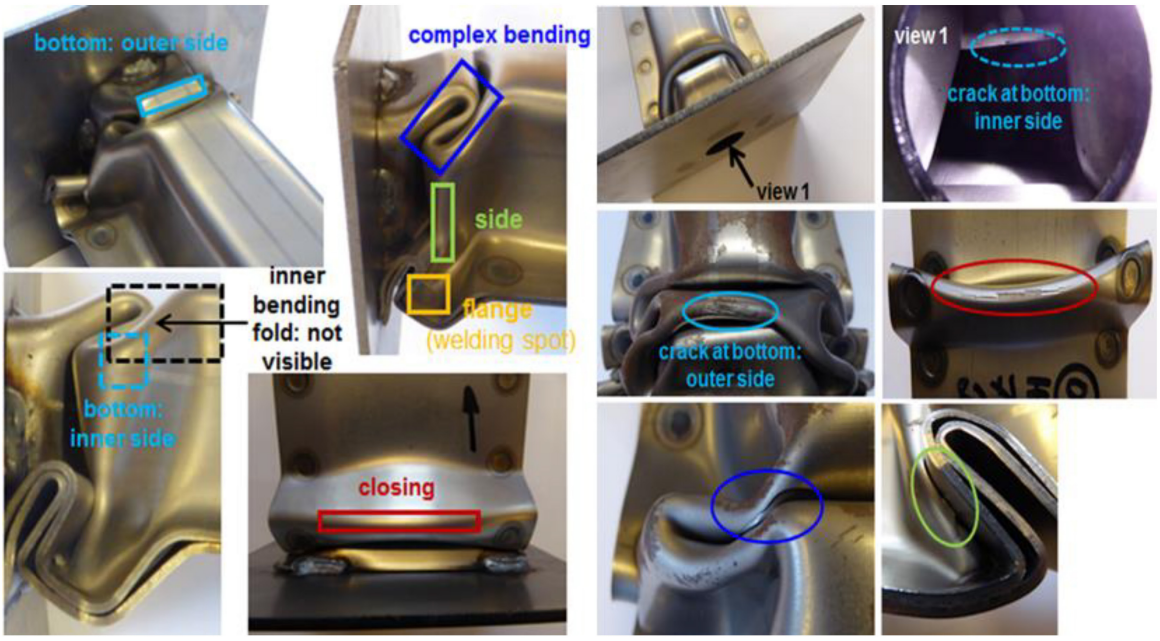

Figure 22 — Observed crack positions on tested axial crash samples [71]

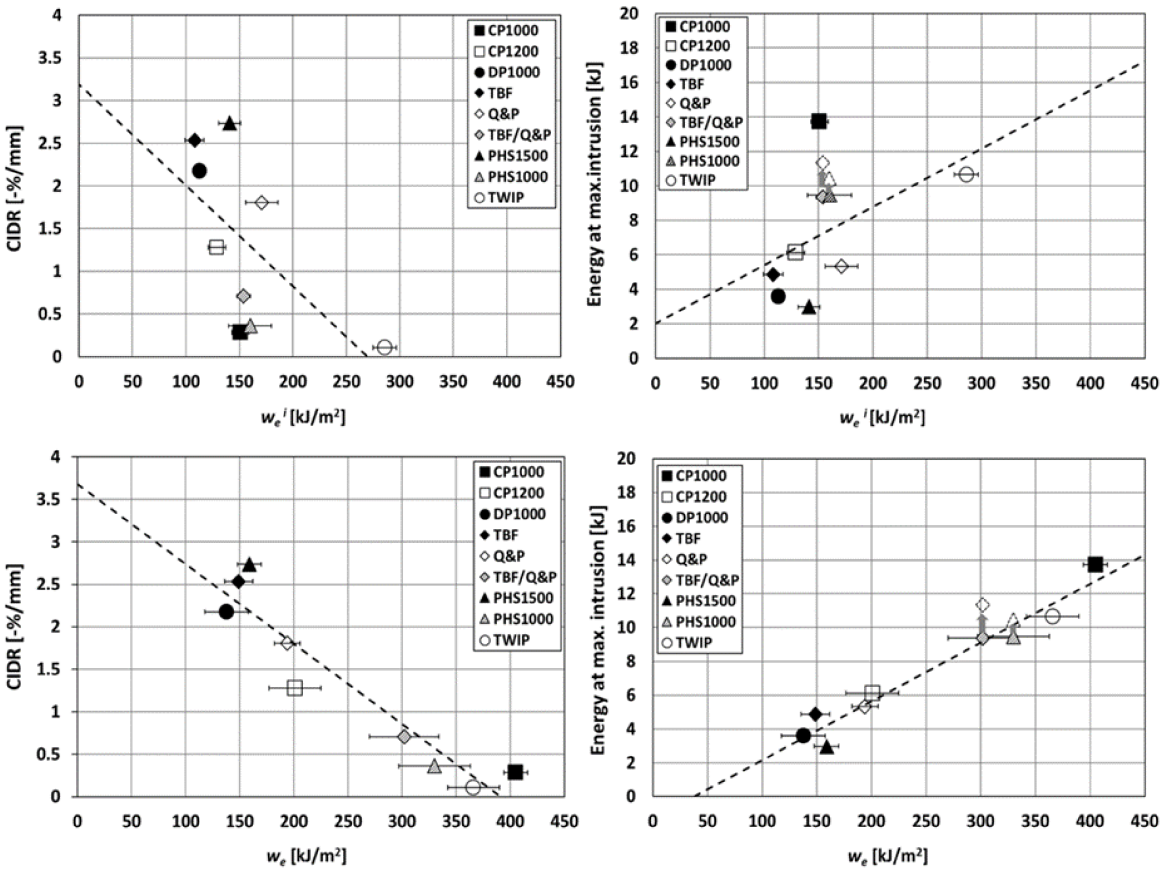

Figure 23 — Crash performance parameters (CIDR in the left and Energy absorbed at maximum intrusion in the right) as a function of fracture toughness parameters ($w_e{}^i$ in the top row and w_e in the bottom row) [71]

7.2 Classification according to cracking resistance

As shown above, the EWF can be a useful tool to better understand the overall fracture resistance of AHSS sheets. According to this, an alternative classification mapping approach was proposed in [56] (Figure 24). In this diagram, uniform elongation (*UE*) is plotted on the horizontal axis and the specific essential work of fracture (w_e) in the vertical axis. *UE* and w_e are used, respectively, as global formability and cracking resistance indices. On that basis, the diagram is divided into different quadrants according to the global formability and cracking resistance level. The more to the right the higher the global formability while upper quadrants indicate superior fracture resistance and damage tolerance. Additionally, an alternative diagram to the traditional "banana" plot is also shown in Figure 25. This classification system provides a more precise description of the fracture resistance of AHSS as a function of their strength level and can serve as a guide for future steel development and material selection.

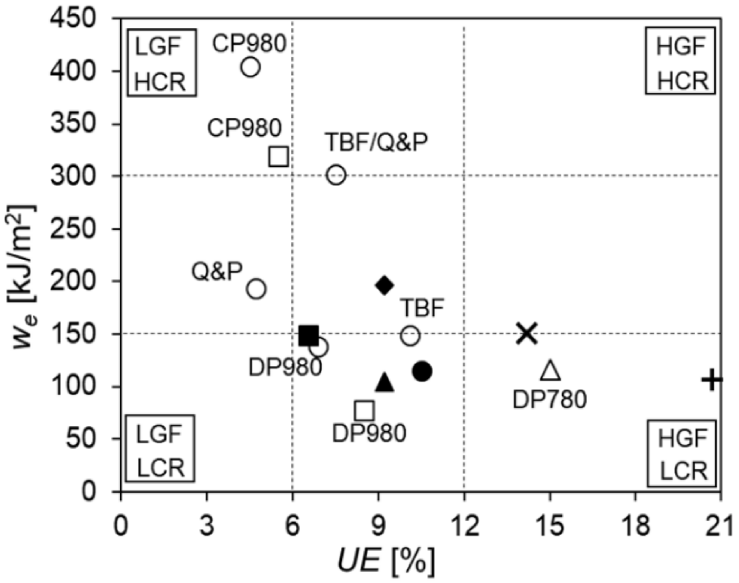

Figure 24 — AHSS classification based on global formability (UE) and fracture resistance (w_e). LGF: low global formability, LCR: low cracking resistance, HGF: high global formability, HCR: high cracking resistance [56]

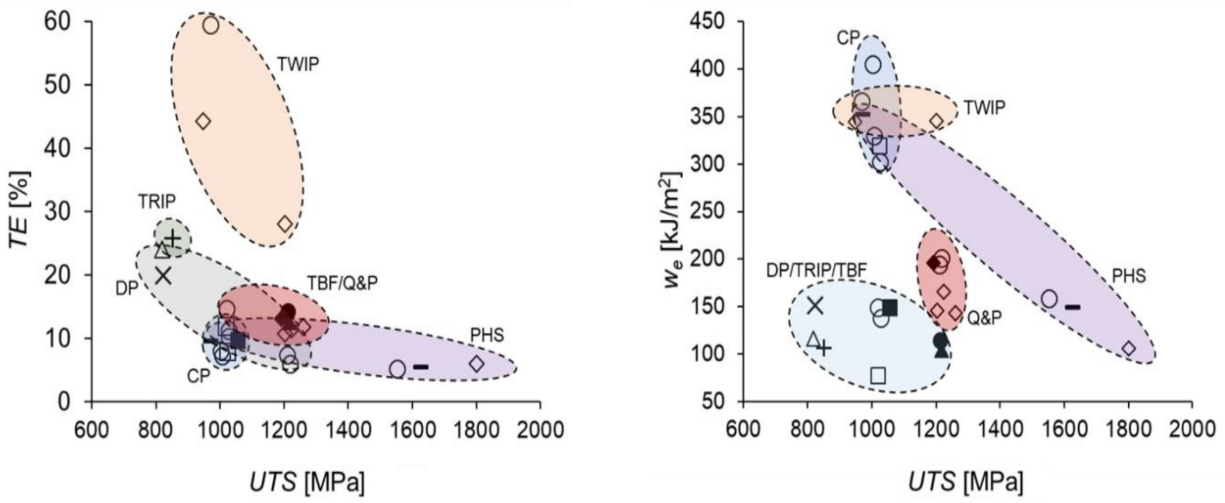

a) **b)**

Figure 25 — a) Conventional classification diagram of AHSS steels ("banana plot") in terms of UTS and TE. b) Proposed diagram for classification of AHSS according to their strength level (UTS) and fracture resistance (w_e) [56]

7.3 Rapid fracture testing methods for material screening

Although the EWF provides relevant information about the fracture resistance of AHSS sheets and is a useful tool for material selection and design, there is still some reticence in the implementation of fracture mechanics techniques at the industrial level. EWF testing is a quite simple method to evaluate the fracture toughness of AHSS sheets and, with the rapid notching procedure described in 5.4.1.3, the tests can be performed in a few minutes. However, the methodology involves the preparation of multiple specimens with different ligament lengths which can make the procedure a bit slower and troublesome for in-plant material control purposes. As explained before, the aim of testing different ligament lengths is to separate the energetic contribution of the essential work of fracture (w_e) developed in the fracture process zone from the plastic energy dissipated around the crack tip (βw_p). The first term is a thickness-dependent material constant that represents the "real" fracture toughness of the material while the second is a geometry-dependent factor associated with plasticity. In other single-specimen methods such as the Kahn-type tear tests this energy partitioning is not possible, which affects the obtained "toughness" values and leads to misleading material ranking [10, 28].

In order to provide an easy-to-measure parameter that allows ranking AHSS according to their crack propagation resistance, a new *Cracking Resistance Index* (*CRI*) was proposed in [85]. The *CRI* is based on the fracture energy obtained from sharp-notched specimens but uses only one ligament length. It is calculated as follows:

$$CRI\,[\%] = \frac{W_{f\,L8}}{UTS \cdot TE \cdot t_0 \cdot l_0^2} \times 100 \tag{16}$$

where

W_{fL8} is the energy under the load-displacement curve of a DENT specimen with ligament length ≈ 8 mm;

UTS is the ultimate tensile strength;

TE is the total elongation;

t_0 is the sheet thickness;

l_0 is the ligament length.

The *CRI* is expressed as a percentage and, as shown in Figure 26, it provides a very similar material ranking to the one obtained using the EWF methodology. This corroborates the validity of the *CRI* as a crack propagation resistance indicator. On the other hand, the use of this index also allows defining different cracking resistance levels for material classification, as illustrated in Figure 26:

— Low cracking resistance (*CRI* ≤ 25 %).

— Medium cracking resistance (25 % < *CRI* ≤ 50 %).

— High cracking resistance (*CRI* > 50 %).

Based on these results, the proposed *CRI* appears to be a useful parameter for material classification and fracture performance estimation of AHSS. It must be emphasized that the *CRI* should be only used as a first approximation for fast material screening but should not replace the proper fracture toughness evaluation of AHSS sheets in the frame of fracture mechanics.

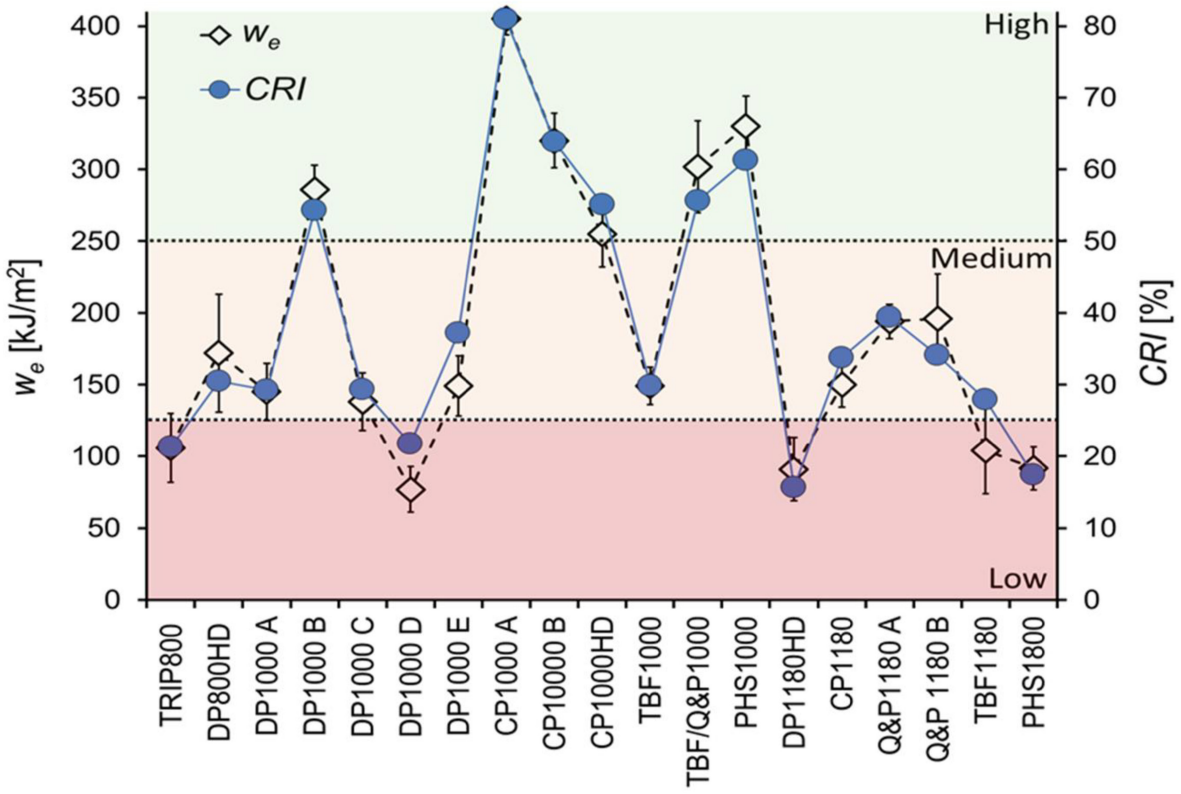

Figure 26 — Comparison of w_e and CRI. The error bars indicate the standard deviation of w_e. Three cracking resistance levels are defined according to the *CRI* [85]

8 Fracture toughness measurements for quality control of raw materials

EWF might also be used as an indicator of coil quality since it is a good method to detect small variations in the local properties of high strength steel coils. Figure 27 and Figure 28 show two examples of how

EWF may help to detect acceptable (OK) and not acceptable (no OK) material batches. Figure 27 shows the values of w_f as a function of the ligament length for two martensitic coils (sheet thickness t=1,6mm), the linear regression obtained using all the data (black solid line) and the standard deviation of the regression line (red and green lines). It can be observed that several points of the NO OK coil are below the standard deviation, which indicates the presence of "low toughness" specimens. The second example (Figure 28) is a case study of the *FormPlanet* project, where EWF tests were performed to discern the different fracture behaviour of thick steel plates (t = 5,0 mm) during fine blanking operations. Figure 28 shows the load-displacement curves obtained for the OK and NO OK batches. Although no large differences were observed in w_f values for the two materials, the load-displacement curves evidenced a different fracture behaviour. As shown in Figure 28 right, the NO OK material presented some specimens with a sudden load drop just after the maximum load, indicating an unstable crack propagation.

These small variations in fracture properties may be associated with a local "embrittlement" due to microstructural heterogeneities, inclusions (number of inclusions, size and/or distribution), etc. and are often difficult to detect by conventional tensile tests. Facture toughness measurements are much more sensitive to small microstructural changes and, thus, provide important information about metallurgical quality.

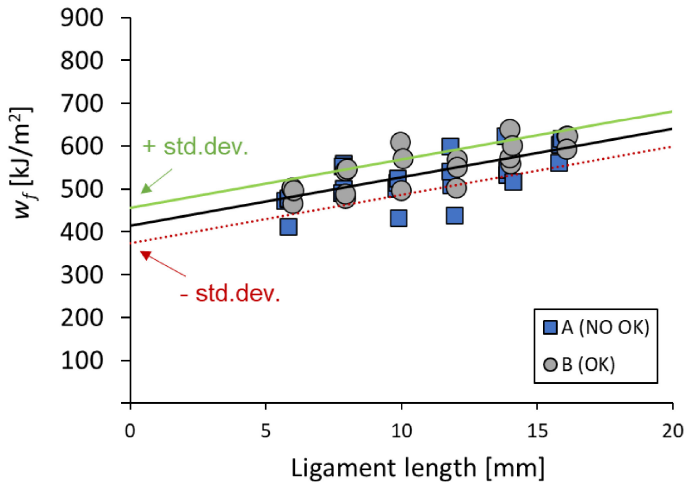

Figure 27 — w_f as a function of the ligament length for OK and NO OK coils of martensitic steel

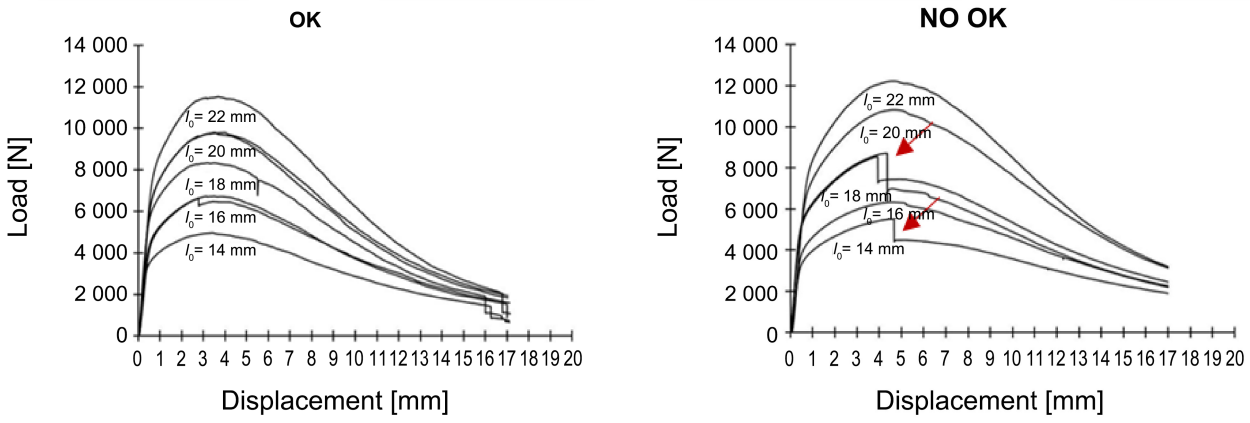

a) **b)**

Figure 28 — Load-displacement curves obtained for two steel batches: OK (a) and NO OK (b)

9 Application of fracture toughness measurements in production: Industrial case studies

A case of industrial applicability of the EWF methodology for edge cracking prediction is presented in [74]. The study was performed in the frame of the RFCS ToughSheet project in collaboration with Centro Ricerche Fiat (CRF). In that study, a serial production automotive component that presented multiple edge cracks was investigated (Figure 29). The component was originally manufactured using a 1 000 MPa Dual Phase (DP) steel of 1,2 mm thickness. After several production problems, it was decided to substitute this material by a Complex Phase (CP) steel showing similar characteristics (same strength and thickness). With the new steel grade, the problems of edge cracking were solved. A first examination of material specifications, including tensile properties and Forming Limit Curves (FLC), did not reveal any apparent cause for the edge cracking problems presented by the DP steel. On the contrary, the material satisfied all the quality requirements and mechanical properties (n value, elongation) and FLC suggested that the DP steel had superior formability (Figure 30 a and b). A more detailed investigation was performed to identify the origin of the poor edge formability of the DP steel. This investigation included hole expansion tests according to ISO 16630 and EWF tests. The results (Figure 30 c and d) confirmed the low fracture toughness of DP1000 compared to CP1000 and the consequent low stretch flangeability, measured by the HER.

The investigations carried out in this work show the potential of the EWF methodology as a tool to select cold forming AHSS grades with improved stretch flangeability and avoid unexpected edge fractures that can slow down the productivity and result in great losses and complications.

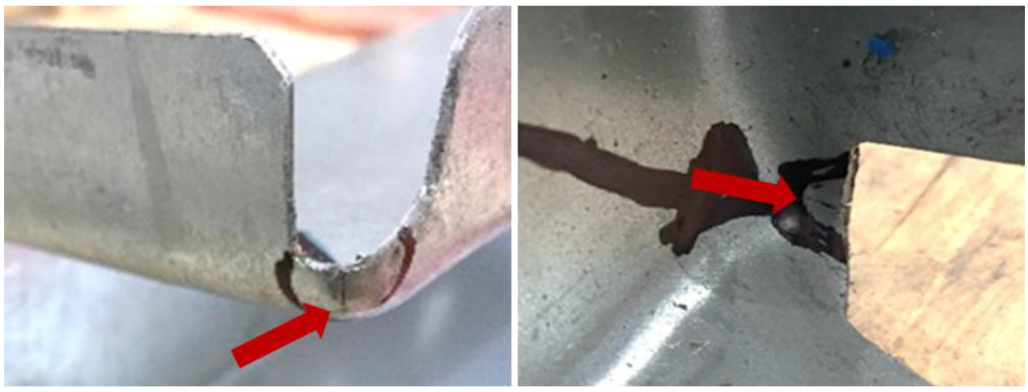

Figure 29 — Edge cracks observed in the component manufactured with DP steel grade [74]

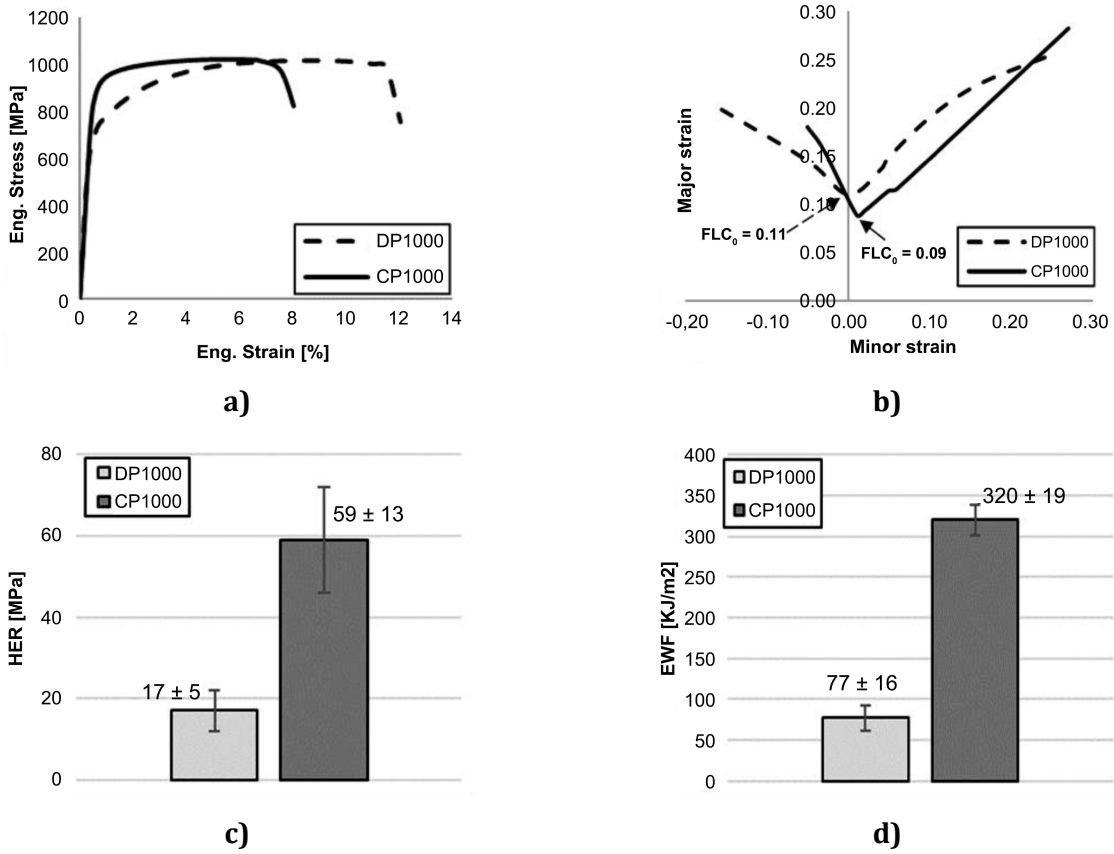

Figure 30 — Results from mechanical characterizations for the investigated CP and DP grades. a) Engineering stress-strain curves, b) FLCs, c) HER and d) EWF. Image from [74]

A similar industrial case study was performed in the H2020 *FormPlanet* project. In that case, the studied component was an automotive part manufactured with a series 5xxx aluminium alloy. The customer detected an increase in the number of rejected parts due to the occurrence of edge fractures in some components (Figure 31). To solve this edge cracking problem, a new material batch with purer chemical composition and a refined manufacturing process was produced. With the new material batch, the edge fracture problem disappeared.

A comparative study was performed to investigate the differences between the old (NO OK) and the new batch (OK). The microstructural and mechanical analysis revealed similar grain size and mechanical properties (Figure 32 a) for both batches. It was observed though that the volume fraction of secondary phases was significantly lower in the OK alloy. The essential work of fracture measurements clearly evidenced the lower fracture toughness of the NO OK batch (Figure 32 b), which shows again the suitability of the EWF methodology to select materials with lower edge fracture sensitivity.

Figure 31 — Edge fracture in a cold-formed automotive component manufactured with a series 5xxx aluminium alloy

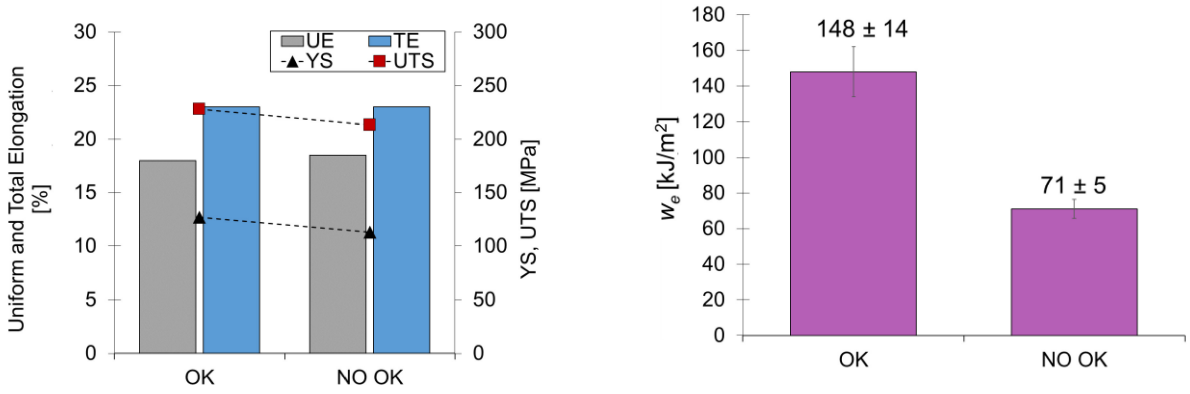

a) **b)**

Figure 32 — a) Mechanical properties obtained for the OK and NO OK batches, b) Fracture toughness results obtained for the OK and NO OK batches

Bibliography

[1] ASTM E1820, *Standard test method for measurement of fracture toughness — American Society for Testing and Materials*

[2] ISO 12135:2016, *Metallic materials — Unified method of test for the determination of quasistatic fracture — International Organization for Standardization*

[3] ASTM E2472, *Standard test method for determination of resistance to stable crack extension under low-constraint conditions — American Society for Testing and Materials*

[4] ISO 22889, Metallic materials — Method of test for the determination of resistance to stable crack extension using specimens of low constraint — *International Organization for Standardization*

[5] Cotterell B., Reddell J.K. The Essential Work of Plane Stress Ductile Fracture. Int. J. Fract. 1977, ••• pp. 267–277

[6] Kaufman J.G., Knoll A.H. Kahn-Type Tear Tests and Crack Toughness of Aluminum Sheet. Metals Research and Standards, 1964, pp. 151–5.

[7] S. Zhang, S. Zhou, M. Li, B. Fu. Calculation and comparison on fracture toughness of specific reliability between ASTM and ISO standards

[8] Xia L., Shih C.F., Hutchinson J.W. A computational approach to ductile crack growth under large scale yielding conditions. J. Mech. Phys. Solids. 1995, 43 pp. 389–413

[9] Zhu X.K., Jang S.K. J-R curves corrected by load-independent constraint parameter in ductile crack growth. Eng. Fract. Mech. 2001, 68 pp. 285–301

[10] Frómeta D., Parareda S., Lara A., Molas S., Casellas D., Jonsén P. et al. Identification of fracture toughness parameters to understand the fracture resistance of advanced high strength sheet steels. Eng. Fract. Mech. 2020, 229 p. 106949

[11] J.L. Arana, J.J. González. Mecánica de fractura. Servicio editorial Universidad del País Vasco

[12] Zhu X.K., Leis B.N. Revisit of ASTM round robin test data for determining R curves of thin sheet materials. J. ASTM Int. 2009, [paper ID JAI102510]

[13] Lacroix G., Pardoen T., Jacques P.J. The fracture toughness of TRIP-assisted multiphase steels. Acta Mater. 2008, 56 pp. 3900–3913

[14] Faccoli M., Cornacchia G., Gelfi M., Panvini A., Roberti R. Notch ductility of steels for automotive components. Eng. Fract. Mech. 2014, 127 pp. 181–193

[15] Marchal Y, Schmidt K, Pardoen T, Knockaert R, Doghri I and Delannay F 1996 Comparison methods for the measurement of fracture toughness of thin sheets: (ECF 11) Mechanisms and Mechanics of Damage and Failure 2259-2265

[16] T. Pardoen, Y. Marchal, F. Delannay. Thickness dependence of cracking resistance in thin aluminium plates. *J. of Mech. Sol.* 47 (1999) 2093-2123

[17] J.C. Newman Jr., M.A. James, U. Zerbst. A review of the CTOA/CTOD fracture criterion. *Eng. Frac. Mech.* 70 (2003) 371-385

[18] J. Heerens, M.Schödel. On the determination of crack tip opening angle, CTOA, using light microscopy and δ_5 measurement technique. *Eng. Frac. Mech.* 70 (2003) 417-426

[19] Koley S., Chatterjee S., Shome M. Evaluation of fracture toughness of thin sheet of interstitial free high strength steel through critical crack tip opening angle (CTOAc) measurement. Int. J. Fract. 2015, 194 pp. 187–195

[20] Xu S., Petri N., Tyson W.R. Evaluation of CTOA from load vs. load-line displacement for C(T) specimen. Eng. Fract. Mech. 2009, 76 (13) pp. 2126–2134

[21] Ben Amara M., Pluvinage G., Capelle J., Azari Z. Crack Tip Opening Angle as a Fracture Resistance Parameter to Describe Ductile Crack Extension and Arrest in Steel Pipes under Service Pressure. Phys. Mesomech. 2015, 18 pp. 355–369

[22] ASTM B871, *Standard Test Method for Tear Testing of Aluminum Alloy Products. American Society for Testing and Materials*

[23] Garret G., Knott J.F. The influence of compositional and microstructural variations on the mechanism of static fracture in aluminum alloys. Metal. Trans. A. 1978, 9 pp. 1187–1201

[24] Dumont D., Deschamps A., Brechet Y. On the relationship between microstructure, strength and toughness in AA7050 aluminum alloy. Mater. Sci. Eng. A. 2003, 356 pp. 326–336

[25] Henn P., Liewald M., Sindel M. Investigation on crashworthiness characterisation of 6xxx series aluminium sheet alloys based on local ductility criteria and edge compression tests. IOP Conf. Ser.: Mater. Sci. Eng. (2018) 418 012125

[26] Ying L., Lu J., Chang Y., Tang X., Hu P., Zhao K. Optimization evaluation test of strength and toughness parameters for hot-stamped high strength steels. J. Iron Steel Res. Int. 2013, 20 pp. 51–56

[27] Lorthios J., Gourgues A.F., Cugy P., Scott C. Damage of TWIP steels for automotive application. ICF12 Int. Conference on Fracture, Ottawa (2009)

[28] Frómeta D., Lara A., Casas B., Casellas D. Fracture toughness measurements to understand local ductility of advanced high strength steels. IOP Conf. Ser.: Mater. Sci. Eng. (2019) 651 012071

[29] Wu J., Mai Y.W. The essential fracture work concept for toughness measurement of ductile polymers. Polym. Eng. Sci. 1996, 36 pp. 2275–2288

[30] Y.W. Mai, B. Cotterell. On the essential work of ductile fracture in polymers. *Int. J. Fract.* 32 (1986) 105-25

[31] Mai Y.W., Powell P. Essential work of fracture and J-integral measurements for ductile polymers. J. Polym. Sci. 1991, 29 pp. 785–793

[32]. Hashemi. Fracture toughness evaluation of ductile polymeric films. J. Mater. Sci. 1997, 32 pp. 1563–1573

[33] Chan W.Y.F., Williams J.G. Determination of the fracture toughness of polymeric films by the essential work method. Polymer (Guildf.). 1994, 35 (8) pp. 1666–1672

[34] León N., Martínez A.B., Castejón P., Arencón D., Martínez P.P. The fracture testing of ductile polymer films: Effect of the specimen notching. Polym. Test. 2017, 63 pp. 180–193

[35] A.B. Martínez, N. León, A. Segovia, J. Cailloux, P.P. Martínez. Effect of specimen notch quality on the essential work of fracture of ductile polymer films. *Engineering Fracture Mechanics* 180 (2017) 296-314

[36] Y.W. Mai, K.M. Pilko. The essential work of plane stress ductile fracture of a strain-aged steel. *J. Mater. Sci.* 14 (1979) 386-394

[37] Marchal Y., Delannay F. Comparison of methods for fracture toughness testing of thin low carbon steel plates. Mater. Sci. Technol. 1998, 14 pp. 1163–1168

[38] Cotterell B., Pardoen T., Atkins A.G. Measuring toughness and the cohesive stress–displacement relationship by the essential work of fracture concept. Eng. Fract. Mech. 2005, 72 pp. 827–848

[39] Marchal Y., Walhin J.F., Delannay F. Statistical procedure for improving the precision of the measurement of the essential work of fracture of thin sheets. Int. J. Fract. 1997, 87 pp. 189–199

[40] Pardoen T., Hachez F., Marchioni B., Blyth P.H., Atkins A.G. Mode I fracture of sheet metal. J. Mech. Phys. Solids. 2004, 52 pp. 423–452

[41] Tuba F., Oláh L., Nagy P. The role of ultimate elongation in the determination of valid ligament range of essential work of fracture tests. J. Mater. Sci. 2012, 47 pp. 2228–2233

[42] Y.W. Mai, B. Cotterell. Effects of pre-strain on plane-stress ductile fracture in α -brass, *J.Mater.Sci.*13 (1980) 2296-2306

[43] Muñoz R., Lara A., Casellas D. Fracture toughness characterization of advanced high strength steels. Int. Deep Drawing Research Group (IDDRG) Conference 2011 (Bilbao, Spain, June 5-8, 2011)

[44] Gutiérrez D., Pérez Ll., Lara A., Casellas D., Prado J.M. Toughness evaluation of high strength steels sheets by means of the essential work of fracture. 19th European conference on fracture: fracture mechanics for durability, reliability and safety, ECF 2012

[45] Casellas D., Lara A., Frómeta D., Gutiérrez D., Molas S., Pérez Ll. et al. Fracture Toughness to Understand Stretch-Flangeability and Edge Cracking Resistance in AHSS. Metall. Mater. Trans., A Phys. Metall. Mater. Sci. 2017, 48 pp. 86–94

[46] Sahoo S., Padmapriya N., De P.S., Chakraborti P.C., Ray S.K. Ductile tearing resistance indexing of automotive grade DP590 steel sheets: EWF testing using DENT specimens. J. Mater. Eng. Perform. 2018, 27 pp. 2018–2023

[47] Sarkara R., Chandra S.K., De P.S., Chakraborti P.C., Ray S.K. Evaluation of ductile tearing resistance of dual-phase DP 780 grade automotive steel sheet from essential work of fracture (EWF) tests. Theor. Appl. Fract. Mech. 2019, 103 p. 102278

[48] S.K. M R. E. Schmidova, P. Konopík, D, Melzer, F. Bozkurt, NV Londe. Fracture Toughness Analysis of Automotive-Grade Dual-Phase Steel Using Essential Work of Fracture (EWF) Method. Metals (Basel). 2020, 10 p. 1019

[49] Ismail K., Perlade A., Jacques P.J., Pardoen T. Outstanding cracking resistance of fibrous dual phase steels. Acta Mater. 2021, 207 p. 116700

[50] Frómeta D., Cuadrado N., Rehrl J., Suppan C., Dieudonné T., Dietsch P. et al. Microstructural effects on fracture toughness of ultra-high strength dual phase sheet steels. Mater. Sci. Eng. A. 2021, 802 p. 140631

[51] Luo Z.C., Liu R.D., Wang X., Huang M.X. The effect of deformation twins on the quasi-cleavage crack propagation in twinning-induced plasticity steels. Acta Mater. 2018, 150 pp. 59–68

[52] Wu R., Li J., Li W., Wu X.C., Jin X., Zhou S. et al. Effect of metastable austenite on fracture resistance of quenched and partitioned (Q&P) sheet steels. Mater. Sci. Eng. A. 2016, 657 pp. 57–63

[53] Golling S., Frómeta D., Casellas D., Jonsén P. Influence of microstructure on the fracture toughness of hot stamped boron steel. Mater. Sci. Eng. A. 2019, 743 pp. 529–539

[54] Broberg K.B. Crack-growth criteria and non-linear fracture mechanics. J. Mech. Phys. Solids. 1971, 19 pp. 407–418

[55] Broberg K.B. On stable crack growth. J. Mech. Phys. Solids. 1975, 23 pp. 215–237

[56] Frómeta D., Lara A., Grifé L., Dieudonné T., Dietsch P., Rehrl J. et al. Fracture resistance of advanced high strength steel sheets for automotive applications. Metall. Mater. Trans., A Phys. Metall. Mater. Sci. 2021, 52 pp. 840–856

[57] Xiong Z., Jacques P.J., Perlade A., Pardoen T. On the sensitivity of fracture mechanism to stress concentration configuration in a two-step quenching and partitioning steel. Int. J. Fract. 2020, 224 pp. 101–116

[58] Hilhorst A., Pardoen T., Jacques P.J. Optimization of the essential work of fracture method for characterization of the fracture resistance of metallic sheets. Eng. Fract. Mech. 2022, 268 p. 108442

[59] Pardoen T. A method for determining the CTOD at cracking initiation – Application to the characterization of the fracture toughness of copper. 13th European Conference on Fracture 2000.

[60] Frómeta D., Lara A., Parareda S., Grifé L., Casellas D. New tool to evaluate the fracture resistance of thin high strength metal sheets. IOP Conf. Ser.: Mater. Sci. Eng. 967 (2020) 012088

[61] Frómeta D. On the measurement of fracture toughness to understand the cracking resistance of Advanced High Strength Steel sheets. PhD thesis, Universitat Politècnica de Catalunya (UPC), 2021

[62] Clutton E. Essential work of fracture. Moore DR, Pavan A, Williams JG, editors. Fracture mechanics testing methods for polymers, adhesives and composites, vol.28. ESIS Publ.; (2001) 177-95

[63] Gray A. Testing protocol for essential work of fracture. ESIS, editor. 1993, European Structural Integrity Society (ESIS) – TC4

[64] Clutton E. Testing protocol for essential work of fracture. ESIS, editor. 1997, European Structural Integrity Society (ESIS) – TC4

[65] Williams J.G., Rink M. The standardisation of the EWF test. Eng. Fract. Mech. 2007, 74 (7) pp. 1009–1017

[66] CWA 17793:2021, *Test method for determination of the EWF of thin ductile metallic sheets.* cwa17793_2021.pdf (cencenelec.eu)

[67] Hance B. Advanced High Strength Steel (AHSS) Performance Levels. SAE Technical Paper 2018-01-0629, 2018

[68] Xiong Z, Jacques PJ, Perlade A, Pardoen T. Characterization and Control of the Compromise Between Tensile Properties and Fracture Toughness in a Quenched and Partitioned Steel. Metall. and Mat. Trans. A (2019)

[69] Larour P., Freudenthaler J., Weissböck T. Reduction of cross section area at fracture in tensile test: measurement and applications for flat sheet steels. J. Phys. Conf. Ser. 2017, 896 p. 012073

[70] Hisker F., Thiessen R., Heller T. Influence of Microstructure on Damage in Advanced High Strength Steels. Mater. Sci. Forum. 2012, 706–709 pp. 925–930

[71] Frómeta D., Lara A., Molas S., Casellas D., Rehrl J., Suppan C. et al. On the correlation between fracture toughness and crash resistance of advanced high strength steels. Eng. Fract. Mech. 2019, 205 pp. 319–332

[72] Jacques P., Furnémont Q., Pardoen T., Delannay F. On the role of martensitic transformation on damage and cracking resistance in trip-assisted multiphase steels. Acta Mater. 2001, 49 pp. 139–152

[73] Krizan D., Steineder K., Kaar S., Hebesberger T. Development of third generation advanced high strength steels for automotive applications. 19th international scientific conference Transfer 2018, Trencianske Teplice (Slovakia)

[74] Frómeta D., Tedesco M., Calvo J., Lara A., Molas S., Casellas D. Assessing edge cracking resistance in AHSS automotive parts by the Essential Work of Fracture methodology. J. Phys. Conf. Ser. 2017, 896 p. 012102

[75] Frómeta D., Lara A., Parareda S., Casellas D. Evaluation of Edge Formability in High Strength Sheets Through a Fracture Mechanics Approach. AIP Conf. Proc. 2019, 2113 p. 160007

[76] Schneider M., Eggers U. 2011 Investigation on punched edge formability Proceedings of International Deep Drawing Research Group 2011 conference (Bilbao, Spain, June 5-8, 2014)

[77] Atzema E., Borsutzki M., Braun M., Brockmann S., Bülter M., Carlsson B. et al. 2012 A European round robin test for the hole expansion test according to ISO 16630 New Development in Sheet Metal Forming, Int. Conf. (Fellbach, Germany, May 23-24, 2012) pp 171-184

[78] Frómeta D, Lara A, Casas B, Casellas D. Fracture toughness measurements to understand local ductility of advanced high strength steels. *IOP Conf. Ser.: Mater. Sci. Eng.* (2019) 651 012071

[79] M.S. Walp MS. Impact Dependent Properties of Advanced and Ultra High Strength Steel. *SAE Technical Paper* 2007-01-0342, 2007

[80] Larour P., Pauli H., Kurz T., Hebseberger T. Influence of post uniform tensile and bending properties on the crash behaviour of AHSS and press-hardening steel grades. Proceedings of the IDDRG2010 (Graz, Austria) 2010

[81] Larour P., Naito J., Pichler A., Kurz T., Murakami T. Side impact crash behavior of press-hardened steels-correlation with mechanical properties. 5th Int. Conf. Hot sheet metal forming of high performance steel (CHS2) (Toronto, Canada, May 31- June 3 2015) pp 281-289

[82] Kurz T., Larour P., Lackner J., Steck T., Jesner G. Press-hardening of zinc coated steel – characterization of a new material for a new process. Proceedings of International Deep Drawing Research Group 2016 Conference (Linz, Austria, June 12-15, 2016)

[83] Link T.M., Hance B.M. Axial and Bending Crash Performance of Advanced High-Strength Steels. Int. Symp. on New Developments in Advanced High-Strength Steels. Keystone, Colorado, USA. 2017

[84] Larour P., Lackner J., Wagner L. Influence of single hat crash box flange triggering and impactor top plate welding strategy on axial crash foldability of AHSS & UHSS sheets. *IOP Conf. Ser.: Mater. Sci. Eng.* 651 012023

[85] Frómeta D., Parareda S., Lara A., Grifé L., Tarhouni I., Casellas D. A new cracking resistance index based on fracture mechanics for high strength sheet metal ranking (2021) I*OP Conf. Ser.: Mater. Sci. Eng*. 1157 012094

[86] ISO 7500-1, *Metallic materials — Verification of static uniaxial testing machines — Part 1: Tension/compression testing machines — Verification and calibration of the force-measuring system*

[87] ISO 9513, *Metallic materials — Calibration of extensometers used in uniaxial testing*

[88] ISO 6892-1, *Metallic materials — Tensile testing — Part 1: Method of test at room temperature*